Establishing High-Fidelity Entanglement in Quantum Repeater Chains

Zhenyu Liu, *Member, IEEE*, Stefano Marano, *Senior Member, IEEE*, and Moe Z. Win, *Fellow, IEEE*

***Abstract*— Entanglement is crucial for many applications such as quantum computing, quantum sensing, and quantum communication. Establishment of entanglement between remote nodes, referred to as remote entanglement establishment (REE), is a key element of the quantum internet. This paper develops a theoretical framework for establishing high-fidelity entanglement between two remote nodes of a quantum repeater chain via entanglement generation, distillation, and swapping operations. In particular, an upper bound on the optimal REE rate under minimum fidelity requirements is established, and an REE policy that achieves such a bound asymptotically is presented. Results in this paper provide guidelines for protocol design in the quantum internet.**

***Index Terms*— Entanglement distribution, entanglement distillation, entanglement swapping, quantum networks.**

I. Introduction

QUANTUM INTERNET is envisioned to provide unprecedented opportunities for computing and communication [1], [2], [3], [4], [5], [6], [7], [8], [9]. Quantum internet is enabled by entanglement [10], [11], [12], a phenomenon in quantum mechanics without classical counterpart. In general, entanglement is a critical resource for many applications in quantum computing [13], [14], [15], [16], [17], [18], [19], quantum sensing [20], [21], [22], [23], [24], [25], [26], [27], and quantum communication [28], [29], [30], [31], [32], [33], [34], [35], [36].

A critical task for enabling quantum internet is establishing entanglement between remote nodes called source nodes and destination nodes. This task is referred to as remote entanglement establishment (REE) or remote entanglement distribution [37], [38], [39], [40], [41], [42]. REE is challenging when the distances between source nodes and destination nodes are large since the quality of the communication channels between the nodes degrades significantly with their distances.

One method for overcoming this challenge is to employ quantum repeater nodes located between the source nodes and the destination nodes. In this method, qubit pairs are first generated among nodes whose distances are smaller than those between the source nodes and the destination nodes. Then, these qubit pairs are consumed for establishing entangled qubit pairs (EQPs) between the source nodes and the destination nodes via entanglement swapping [43], [44], [45]. The quality of the EQPs can be described by their fidelity with respect to maximally entangled quantum states [46], [47], [48]. Since quantum swapping typically degrades fidelity, the qubit pairs established via swapping may not satisfy the fidelity requirement. One technique for addressing this issue is to perform entanglement distillation [49], [50], [51], before and/or after entanglement swapping. One class of influential entanglement distillation protocols is that of recurrence protocols [52], [53], [54], where quantum operations are performed on each two qubit pairs to obtain one qubit pair with higher fidelity while the other qubit pair is discarded.

REE has been studied in existing works [55], [56], [57], [58], [59]. These works typically assume that quantum states in REE remain maximally entangled, i.e., their fidelity remains one, and thus the effects of quantum operations on fidelity are not considered. There are some works that do not make such an assumption and account for requirements on the fidelity of EQPs [60], [61], [62]. Among these works that account for fidelity requirements, most do not consider entanglement distillation and impose constraints on the maximum number of swapping operations in order to meet the fidelity requirements. Another limitation of the existing literature is that some works only consider a particular order for entanglement swapping on repeater chains, a technique referred to as "doubling," and disregard other possible swapping orders. As a result, a methodology for REE that accounts for both entanglement distillation and swapping operations and that considers all possible orders of swapping is still lacking.

A fundamental question for REE is: what is the optimal rate at which entanglement can be established between remote nodes while ensuring that the established EQPs satisfy the fidelity requirements? The answer to this question will enable the design of efficient REE policies for quantum internet. This paper aims to develop a theoretical framework for establishing high-fidelity entanglement in quantum repeater chains. In order to develop such a framework, we advocate to use the

Manuscript received 2 June 2023; revised 3 December 2023; accepted 20 December 2023. Date of publication 8 April 2024; date of current version 19 June 2024. The fundamental research described in this paper was supported, in part, by the National Science Foundation under Grant No. CCF-1956211 and by the MIT Institute for Soldier Nanotechnologies. An earlier version of this paper was presented in part at the 2024 IEEE International Conference on Acoustics, Speech, and Signal Processing, Seoul, South Korea. *(Corresponding author: Moe Z. Win.)*

Zhenyu Liu is with the Wireless Information and Network Sciences Laboratory, Massachusetts Institute of Technology, Cambridge, MA 02139 USA.

Stefano Marano is with the Department of Information & Electrical Engineering and Applied Mathematics, University of Salerno, 84084 Fisciano (SA), Italy.

Moe Z. Win is with the Laboratory for Information and Decision Systems, Massachusetts Institute of Technology, Cambridge, MA 02139 USA (e-mail: moewin@mit.edu).

Color versions of one or more figures in this article are available at https://doi.org/10.1109/JSAC.2024.3380092.

Digital Object Identifier 10.1109/JSAC.2024.3380092

TABLE I
NOTATION AND DEFINITIONS OF SOME MATHEMATICAL QUANTITIES

Notation	Definition	Notation	Definition
L	length of the quantum repeater chain	$w^{l-1,l}$	fidelity of CQPs between nodes $l-1$ and l
q	success probability of entanglement swapping	$g_{\mathrm{s}}(w,w')$	fidelity of qubit pair obtained via successful swapping that consumes two qubit pairs with fidelities w and w'
$p_{\mathrm{d}}(w)$	probability of successfully creating one distilled qubit pair consuming two qubit pairs each with fidelity w	$g_{\mathrm{d}}(w)$	fidelity of qubit pair obtained via successful distillation that consumes two qubit pairs each with fidelity w
$\mathrm{s}^{i,j,l}$	perform one round of swapping between nodes i and l at node j	$\mathrm{d}^{i,j}$	perform one round of distillation between nodes i and j
$\mathbf{d}_c^{i,j}$	perform c rounds of distillation between nodes i and j	$b^{l-1,l}$	budget of CQPs for the link between nodes $l-1$ and l
$\underline{w}$	EQP fidelity threshold	$\boldsymbol{b}$	CQP budget vector
$\boldsymbol{w}$	CQP fidelity vector	π	REE policy, i.e., a sequence of entanglement generation, distillation, and swapping operations
$\mathsf{z}_\pi(\boldsymbol{b},\boldsymbol{w})$	number of EQPs established via policy π for CQP budget vector $\boldsymbol{b}$ and CQP fidelity vector $\boldsymbol{w}$	$r_\pi(\boldsymbol{b},\boldsymbol{w})$	REE rate of policy π for CQP budget vector $\boldsymbol{b}$ and CQP fidelity vector $\boldsymbol{w}$
$r^*(\boldsymbol{b},\boldsymbol{w})$	optimal REE rate for CQP budget vector $\boldsymbol{b}$ and CQP fidelity vector $\boldsymbol{w}$	$\mathrm{e}_c^{i,j}$	enode representing qubit pairs between nodes i and j obtained after c rounds of distillations over link (i,j)
$\mathcal{G}_{\mathrm{e}}$	enode graph, which is a directed acyclic graph with enodes as its vertices	$\boldsymbol{u}$	REE procedure
$g_{\boldsymbol{u}}(\boldsymbol{w})$	fidelity of qubit pairs successfully established by performing REE procedure $\boldsymbol{u}$ for CQP fidelity vector $\boldsymbol{w}$	$\boldsymbol{n}$	CQP number vector
$\check{\mathsf{z}}_{\boldsymbol{u}}(\boldsymbol{n},\boldsymbol{w})$	number of EQPs established by performing REE procedure $\boldsymbol{u}$ for CQP number vector $\boldsymbol{n}$ and CQP fidelity vector $\boldsymbol{w}$	$\zeta_{\boldsymbol{u}}(\boldsymbol{n},\boldsymbol{w})$	number of EQPs established by performing REE procedure $\boldsymbol{u}$ under CE for CQP number vector $\boldsymbol{n}$ and CQP fidelity vector $\boldsymbol{w}$
$\boldsymbol{v}_{\boldsymbol{u}}(\boldsymbol{w})$	allocation vector for REE procedure $\boldsymbol{u}$ and CQP fidelity vector $\boldsymbol{w}$	$\boldsymbol{u}^{(m)}$	mth efficient REE procedure for a given fidelity vector and EQP fidelity threshold

techniques of certainty equivalence and linear programming for determining the performance limits of REE.

In this paper, we derive an upper bound of the optimal REE rates for quantum repeater chains. This bound is shown to be asymptotically achievable when the number of qubit pairs generated over each elementary link is sufficiently large. The key contributions of this paper are as follows:

- we present a general model for REE via entanglement generation, distillation, and swapping accounting for each operation's effects on the fidelity of qubit pairs;
- we derive an upper bound of the optimal REE rate under the requirement that the fidelity of EQPs exceeds a desired threshold; and
- we design an REE policy that achieves the derived upper bound asymptotically and validate the designed policy via simulation.

The remaining sections of the paper are organized as follows. Section II presents the system model. Section III presents the upper bound on the optimal REE rate and the design of REE policy. Section IV presents numerical results. Section V concludes the paper.

Notation: Random variables are displayed in sans serif, upright fonts; their realizations in serif, italic fonts. Vectors and matrices are denoted by bold lowercase and uppercase letters, respectively. For example, a random variable and its realization are denoted by x and x, respectively; a random vector and its realization are denoted by $\mathbf{x}$ and $\boldsymbol{x}$, respectively. The expectation of $\mathbf{x}$ is denoted by $\mathbb{E}\{\mathbf{x}\}$, whereas the conditional expectation of $\mathbf{x}$ given $\mathbf{y}$ is denoted by $\mathbb{E}\{\mathbf{x}\,|\,\mathbf{y}\}$. A random variable x following the binomial distribution with n trials and success probability p of each trial is denoted by $\mathsf{x}\sim\mathrm{Bin}(n,p)$. The sets of real numbers and non-negative integers are denoted by $\mathbb{R}$ and $\mathbb{N}$, respectively. The composition of m copies of function f is denoted by $f^{\circ m}$ for a positive integer m. For example, $f^{\circ 1}(\cdot):=f(\cdot)$, and $f^{\circ 2}(\cdot):=f\big(f(\cdot)\big)$. Moreover, $f^{\circ 0}$ is defined as the identity mapping on real numbers, i.e., $f^{\circ 0}(x):=x$ for all $x\in\mathbb{R}$. For non-negative integers i and j with $i\leqslant j$, notation $i\colon j$ represents the sequence $(i,i+1,\ldots,j)$. Given an n-dimensional vector $\boldsymbol{x}$, a vector consisting of its ith entry to jth entry is denoted by $[\boldsymbol{x}]_{i:j}$ for $1\leqslant i\leqslant j\leqslant n$. The ℓ_1 norm of vector $\boldsymbol{x}$ is denoted by $|\boldsymbol{x}|$. The relationship that vector $\boldsymbol{x}_1$ is larger than or equal to (resp. smaller than or equal to) vector $\boldsymbol{x}_2$ entry-wise is represented by $\boldsymbol{x}_1\succcurlyeq\boldsymbol{x}_2$ (resp. $\boldsymbol{x}_1\preccurlyeq\boldsymbol{x}_2$). The vector of zeros (resp. ones) is denoted by $\mathbf{0}$ (resp. $\mathbf{1}$). The floor function is denoted by $\lfloor\cdot\rfloor$, i.e., $\lfloor x\rfloor$ represents the largest integer smaller than or equal to $x\in\mathbb{R}$. Given a vector $\boldsymbol{x}$, notation $\lfloor\boldsymbol{x}\rfloor$ represents a vector obtained by applying floor function to each entry of $\boldsymbol{x}$. Notation and definitions for some mathematical quantities used in the paper are summarized in Table I. Acronyms and their expansions used in the paper are summarized in Table II.

II. SYSTEM MODEL

This section introduces the network model, presents quantum operations for a single qubit pair and for multiple qubit pairs, and describes the objective of REE. The model described in this section is the same as that presented in [63].

A. Network Model

Consider a quantum repeater chain (or chain for short) consisting of $L+1$ nodes identified by indices $0,1,\ldots,L$,

TABLE II
EXPANSIONS OF ACRONYMS

Acronym	Expansion	Acronym	Expansion
REE	remote entanglement establishment	EQP	entangled qubit pair
CQP	crude qubit pair	DAG	directed acyclic graph
CE	certainty equivalence	QKD	quantum key distribution

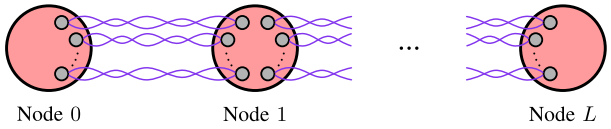

Fig. 1. Quantum repeater chain consisting of nodes identified by indices $0, 1, \ldots, L$. A qubit pair between two neighbor nodes, i.e., over an elementary link, is represented by two grey dots connected by two curly purple lines.

as shown in Figure 1. The number L is referred to as the length of the chain. Two nodes identified by consecutive indices $l-1$ and l for $l = 1, 2, \ldots, L$ are referred to as neighbors. Nodes of the chain can be visualized as points on a horizontal line such that node $l-1$ lies immediately to the left of node l. The aim of REE is to establish EQPs between the source node 0 and the destination node L via quantum operations including entanglement generation, entanglement distillation, and entanglement swapping.

B. Quantum Operations Establishing a Single Qubit Pair

Entanglement generation, entanglement distillation, and entanglement swapping for a single qubit pair are described in the following.

- Entanglement generation: for $1 \leqslant l \leqslant L$, create a qubit pair called crude qubit pair (CQP) between nodes $l-1$ and l. In particular, the density operator $\boldsymbol{\Xi}^{l-1,l}$ describing the CQP shared by nodes $l-1$ and l is given by

$$\boldsymbol{\Xi}^{l-1,l} := w^{l-1,l}\big|\boldsymbol{\phi}^+\rangle\langle\boldsymbol{\phi}^+\big| + (1-w^{l-1,l})\big|\boldsymbol{\psi}^+\rangle\langle\boldsymbol{\psi}^+\big| \tag{1}$$

  where $1/2 < w^{l-1,l} \leqslant 1$ is a scalar representing the fidelity of (1) with respect to density operator $\big|\boldsymbol{\phi}^+\rangle\langle\boldsymbol{\phi}^+\big|$. All fidelities considered in this paper are computed with respect to $\big|\boldsymbol{\phi}^+\rangle\langle\boldsymbol{\phi}^+\big|$. Here and in (1), $\big|\boldsymbol{\phi}^+\big\rangle$ and $\big|\boldsymbol{\psi}^+\big\rangle$ are pure Bell states given by

$$\big|\boldsymbol{\phi}^+\big\rangle := \frac{1}{\sqrt{2}}\big(\big|00\big\rangle + \big|11\big\rangle\big)$$
$$\big|\boldsymbol{\psi}^+\big\rangle := \frac{1}{\sqrt{2}}\big(\big|01\big\rangle + \big|10\big\rangle\big)$$

  where $\{\big|00\big\rangle, \big|01\big\rangle, \big|10\big\rangle, \big|11\big\rangle\}$ represents the computational basis for two-qubit systems. Note that the CQP is in mixed Bell state in general, and the CQP becomes the pure state $\big|\boldsymbol{\phi}^+\big\rangle$ for the special case $w^{l-1,l} = 1$.
- Entanglement distillation: for $0 \leqslant i < j \leqslant L$, consume two qubit pairs between nodes i and j to generate one qubit pair called a distilled qubit pair. This operation is referred to as entanglement distillation between nodes i and j. Entanglement distillation can fail and the success probability of distillation is determined by the fidelity of the consumed qubit pairs. Specifically, the probability of successfully creating one distilled qubit pair consuming two qubit pairs with fidelity w is $p_{\mathrm{d}}(w)$ given by [53]

$$p_{\mathrm{d}}(w) := w^2 + (1-w)^2. \tag{2}$$

  If the distillation operation is successful, the fidelity $g_{\mathrm{d}}(w)$ of the distilled qubit pair is given by [53]

$$g_{\mathrm{d}}(w) := \frac{w^2}{w^2 + (1-w)^2}. \tag{3}$$

  It holds that $g_{\mathrm{d}}(w) \geqslant w$ for any $1/2 < w \leqslant 1$, with equality achieved if and only if $w = 1$. This shows that distillation increases fidelity, which comes at the cost of the number of qubit pairs. Entanglement distillation can be performed recursively. That is to say, two distilled qubit pairs can be consumed to create one qubit pair with even higher fidelity via entanglement distillation.
- Entanglement swapping: for $0 \leqslant i < j < l \leqslant L$, consume one qubit pair between nodes i and j and one qubit pair between nodes j and l to create one qubit pair called a swapped qubit pair between nodes i and l. This operation is referred to as entanglement swapping between nodes i and l at node j. Entanglement swapping can fail and the success probability of swapping one qubit pair between nodes i and l is denoted by q with $0 < q \leqslant 1$. The fidelity of the successfully swapped qubit pair is determined by those of the consumed qubit pairs. Specifically, let w represent the fidelity of the qubit pair between nodes i and j, and let w' represent the fidelity of the qubit pair between nodes j and l. If the swapping operation is successful, the fidelity $g_{\mathrm{s}}(w, w')$ of the swapped qubit pair is given by [43]

$$g_{\mathrm{s}}(w, w') := ww' + (1-w)(1-w'). \tag{4}$$

  It holds that $g_{\mathrm{s}}(w, w') \leqslant \min\{w, w'\}$ for any $1/2 < w, w' \leqslant 1$, with equality achieved if and only if $w = 1$ or $w' = 1$. This shows that swapping reduces fidelity.

The entanglement generation operation and the density operator $\boldsymbol{\Xi}^{l-1,l}$ for the CQPs are explained as follows. Consider the entanglement generation operation over an elementary link $(l-1, l)$. First, node $l-1$ prepares a Bell state $\big|\boldsymbol{\phi}^+\big\rangle$ locally. Then, node $l-1$ keeps the first qubit of the Bell state and sends the second qubit to node l via a quantum channel. The qubit kept by node $l-1$ and the qubit received by node l constitute a remote qubit pair. Due to the quantum channel, the remote qubit pair becomes a mixed state and its fidelity falls below one. In particular, if the quantum channel is a bit flip channel [46], then the remote qubit pair can be written as the right-hand side of (1). Such a remote qubit

pair is a CQP obtained via entanglement generation. For more general quantum channels such as two-Kraus-operator channels, we consider the scenario where the adaptive technique proposed in [53] is employed to mitigate the negative effect of the channel. The intermediate outcomes of such an adaptive technique are viewed as CQPs and their density operator can be written as in (1). Specifically, the adaptive technique proposed in [53] consists of three steps: remote shared-state preparation (RSSP), first round of distillation, and following rounds of distillation. The RSSP step consists of local unitary operations, quantum measurement, and classical communication. The first round of distillation and following rounds of distillation are the same as the entanglement distillation operation described earlier in this paper. We view the concatenation of RSSP and the first round of distillation as the entanglement generation operation. Consequently, the qubit pairs successfully distilled by the first round of distillation are CQPs. The density of these CQP can be written as in (1) [53, Appendix F]. Note that the following rounds of distillation in the adaptive technique are viewed as entanglement distillation operations and not part of entanglement generation.

Both entanglement distillation and swapping operations are critical for REE. In particular, entanglement distillation is performed in order to ensure that the EQPs satisfy the fidelity requirement. The significance of entanglement swapping can be seen by regarding qubit pairs between node i and node j as a link between the two nodes. This link is denoted by (i,j) and the length of the link is defined to be $|j-i|$. For the case that $|j-i|=1$, the link (i,j) is referred to as an elementary link. REE aims to create a link of length L, whereas entanglement generation can only create links of length 1. Entanglement swapping creates longer links by consuming qubit pairs on shorter links so that REE can be achieved.

Quantum operations described in this section require quantum memories for storing the qubit pairs created by entanglement generation, distillation, and swapping. Qubit pairs decohere as they are stored in the memory and their fidelities decrease with time due to the interaction with the environment [64], [65], [66]. The amount of time for which the fidelity of qubit pairs does not decrease significantly as they stay in memory is referred to as memory coherence time. One method for mitigating the effects of memory decoherence is to perform memory cutoff, namely discarding qubit pairs that have stayed in the memory for a long time compared to the memory coherence time or discarding qubit pairs whose fidelities have dropped significantly [67], [68], [69]. In this paper, we consider scenarios in which quantum memories with large coherence times are employed by the repeater chain so that the decoherence is insignificant. Indeed, quantum memories with large memory coherence times have been reported in the literature. For example, quantum memories realized via silicon-vacancy centers, ions, and atoms can achieve memory coherence time of tens of microseconds [70]. For scenarios in which decoherence is non-negligible, the REE rates would decrease. Consequently, the upper bounds derived in this paper still hold but become difficult to achieve.

C. Quantum Operations Establishing Multiple Qubit Pairs

Quantum operations described in Section II-B can be performed for multiple qubit pairs. Specifically, multiple qubit pairs can be created over a link $(l-1,l)$ via entanglement generation. The density operators of the generated qubit pairs are all given by (1) and thus they have the same fidelity.

Entanglement distillation can be performed on multiple qubit pairs. Suppose that there are $n^{i,j}$ qubit pairs between nodes i and j, each with fidelity $w^{i,j}$. Then $n^{i,j}$ qubit pairs can be consumed to create distilled qubit pairs between nodes i and j. This quantum operation is called performing "one round of distillation between nodes i and j" and is denoted by $\mathrm{d}^{i,j}$. The number of qubit pairs created by $\mathrm{d}^{i,j}$ is a random variable determined by the success of the distillation operation for each qubit pair between nodes i and j. In particular, the successes of distillation for different qubit pairs are assumed independent, and thus the number of qubit pairs created by $\mathrm{d}^{i,j}$ follows a binomial distribution given by

$$\mathrm{Bin}\Big(\Big\lfloor\frac{n^{i,j}}{2}\Big\rfloor, p_{\mathrm{d}}\big(w^{i,j}\big)\Big)$$

where $p_{\mathrm{d}}(\cdot)$ is given in (2). The fidelity of these successfully distilled qubit pairs is $g_{\mathrm{d}}\big(w^{i,j}\big)$, where $g_{\mathrm{d}}(\cdot)$ is given in (3).

As mentioned in Section II-B, rounds of entanglement distillation can be performed recursively. Specifically, the qubit pairs created by performing one round of entanglement distillation between nodes i and j can be consumed to perform another round of distillation in order to further improve the fidelity of the distilled qubit pairs. This is called performing "two rounds of distillation between nodes i and j." The operation of performing c rounds of distillation between nodes i and j can be defined for $c\in\mathbb{N}$. Such an operation can be represented by a sequence consisting of c copies of $\mathrm{d}^{i,j}$ and is denoted by $\mathbf{d}_c^{i,j}$ for short. In this paper, all the qubit pairs that are consumed in the cth round of distillation are those successfully created in the $(c-1)$th round of distillation for $c\geqslant 2$, whereas all the qubit pairs that are consumed in the first round of distillation are CQPs. As a result, all the qubit pairs consumed in a certain round of distillation have the same fidelity. This is a typical assumption for recurrence entanglement distillation protocols. There are entanglement distillation protocols such as the entanglement pumping protocol [61] where qubit pairs with different fidelities are consumed in a certain round of distillation. These protocols are typically less efficient for achieving a given level of fidelity compared to recurrence protocols and are not considered in this paper [71].

Entanglement swapping can also be performed on multiple qubit pairs. Suppose that there are $n^{i,j}$ qubit pairs between nodes i and j, each with fidelity $w^{i,j}$, whereas there are $n^{j,l}$ qubit pairs between nodes j and l, each with fidelity $w^{j,l}$. Then $\min\{n^{i,j},n^{j,l}\}$ qubit pairs between nodes i and j, together with the same number of qubit pairs between nodes j and l, can be consumed to create qubit pairs between nodes i and l via entanglement swapping. This quantum operation is called performing "one round of swapping between nodes i and l at node j" and is denoted by $\mathrm{s}^{i,j,l}$. The number of qubit pairs created by $\mathrm{s}^{i,j,l}$ is a random variable determined by the success of the swapping operation for each qubit pair between nodes

i and l at node j. In particular, the successes of swapping for different qubit pairs are assumed independent, and thus the number of qubit pairs created by $\mathrm{s}^{i,j,l}$ follows a binomial distribution given by

$$\mathrm{Bin}\big(\min\{n^{i,j}, n^{j,l}\},\, q\big)\,.$$

The fidelity of these successfully swapped qubit pairs is $g_{\mathrm{s}}\big(w^{i,j}, w^{j,l}\big)$, where $g_{\mathrm{s}}(\cdot,\cdot)$ is given in (4).

D. Objective of REE

The aim of REE is to create EQPs between node 0 and node L with acceptable fidelity via the quantum operations described in Section II-B. Specifically, a qubit pair established between these two nodes is referred to as an EQP if its fidelity is above a given threshold $\underline{w} > 1/2$. Note that a threshold for the fidelity of EQPs is employed since, in many applications, a qubit pair whose fidelity is low may not be useful. For example, it has been shown that in the application of secure quantum key distribution (QKD) on repeater chains, the secret-key rate drops to zero, i.e., no secure quantum key can be distributed, if the fidelity of the qubit pairs between the two parties aiming to create private keys falls below certain values [72], [73], [74]. The value of $\underline{w}$ can be determined based on the applications that the EQPs are used for. For example, $\underline{w}$ can be chosen to maximize secret key rates accounting for tradeoffs between raw key rates and secret fractions. Specifically, the secret key rate is the product of the raw key rate with the secret fraction [75]. On the one hand, setting a high $\underline{w}$ would decrease the raw key rate as more entanglement distillation operations are required to meet the fidelity requirement. On the other hand, setting a high $\underline{w}$ would increase the secret fraction as entanglement with higher fidelities are used for QKD. The expressions of raw key rates and secret fractions as functions of the fidelities of entanglement depend on REE protocols and QKD protocols. Such expressions can be found in [67], [71], and [76].

The objective function of REE, named REE rate, is described as follows. Each elementary link is given a budget on the number of CQPs it can generate. The objective is to maximize the expected number of established EQPs between nodes 0 and L by designing an REE policy, which contains a sequence of entanglement generation, distillation, and swapping operations. Specifically, for $l = 1, 2, \ldots, L$, let $b^{l-1,l}$ represent the budget of CQPs for the elementary link $(l-1, l)$, and let $w^{l-1,l}$ represent the fidelity of the CQPs generated on this link. Moreover, define CQP budget vector $\boldsymbol{b}$ and CQP fidelity vector $\boldsymbol{w}$ as

$$\boldsymbol{b} := \begin{bmatrix} b^{0,1} & b^{1,2} & \cdots & b^{L-1,L} \end{bmatrix}^{\mathrm{T}} \tag{5a}$$

$$\boldsymbol{w} := \begin{bmatrix} w^{0,1} & w^{1,2} & \cdots & w^{L-1,L} \end{bmatrix}^{\mathrm{T}}. \tag{5b}$$

Given $\boldsymbol{b}$ and $\boldsymbol{w}$, the number of EQPs established between nodes 0 and L via a policy π is a random variable denoted by $\mathsf{z}_\pi(\boldsymbol{b}, \boldsymbol{w})$. Define the REE rate $r_\pi(\boldsymbol{b}, \boldsymbol{w})$ of policy π as the ratio between the expectation of $\mathsf{z}_\pi(\boldsymbol{b}, \boldsymbol{w})$ and the average CQP budget $|\boldsymbol{b}|/L$ among all elementary links, i.e.,

$$r_\pi(\boldsymbol{b}, \boldsymbol{w}) := \frac{L}{|\boldsymbol{b}|}\mathbb{E}\big\{\mathsf{z}_\pi(\boldsymbol{b}, \boldsymbol{w})\big\}\,.$$

Note that $0 \leqslant r_\pi(\boldsymbol{b}, \boldsymbol{w}) \leqslant 1$ for any policy π, since

$$0 \leqslant \mathsf{z}_\pi(\boldsymbol{b}, \boldsymbol{w}) \leqslant \min\big\{b^{0,1}, b^{1,2} \cdots b^{L-1,L}\big\} \leqslant |\boldsymbol{b}|/L\,.$$

The optimal REE rate $r^*(\boldsymbol{b}, \boldsymbol{w})$ is defined as the maximum of the REE rates over all policies, i.e.,

$$r^*(\boldsymbol{b}, \boldsymbol{w}) := \max_{\pi}\, r_\pi(\boldsymbol{b}, \boldsymbol{w})\,. \tag{6}$$

This paper aims to derive an upper bound on $r^*(\boldsymbol{b}, \boldsymbol{w})$ and to design REE policies whose rates approach this bound.

Investigating $r^*(\boldsymbol{b}, \boldsymbol{w})$ is a challenging task since there are multiple manners in which entanglement can be established. To explain the challenges, the notion of REE procedures defined in Section III is used. An REE procedure is a sequence of entanglement distillation and swapping operations. For a repeater chain, an efficient REE policy typically involves selecting different REE procedures, allocating a proportion of the CQP budget to each selected REE procedure, generating CQPs according to the allocated budget, and consuming these CQPs to perform the quantum operations specified by that REE procedure. For example, consider a chain of length $L = 3$ and assume that the fidelities of the CQPs are sufficiently high so that no distillation is needed to satisfy the fidelity requirement. There are two REE procedures for establishing entanglement between nodes 0 and 3. The first REE procedure consists of $\mathrm{s}^{0,1,2}$ and $\mathrm{s}^{0,2,3}$, namely performing swapping between nodes 0 and 2 at node 1 first, then performing swapping between nodes 0 and 3 at node 2. The second REE procedure consists of $\mathrm{s}^{1,2,3}$ and $\mathrm{s}^{0,1,3}$, namely swapping between nodes 1 and 3 at node 2 first, then swapping between nodes 0 and 3 at node 1. An efficient REE policy may select both procedures, allocate part of the CQP budget to each REE procedure, and perform the quantum operations according to the selected REE procedure. As the chain becomes longer and as distillation operations need to be included in REE procedures, the number of REE procedures becomes significantly larger. As a result, selecting REE procedures and allocating the CQP budget efficiently become more difficult.

Some comments that compare the terminology used in this paper with that in the literature are in order. In some existing works on quantum networks, CQPs are referred to as link-level entanglements, whereas EQPs are referred to as end-to-end entanglements [77], [78], [79]. In this paper, CQP is used to emphasize that the fidelities of qubit pairs generated over elementary links may be low and thus entanglement distillation operations are required. Moreover, EQP is used to emphasize that the fidelities of qubit pairs between the source node and destination node are required to exceed a given threshold.

III. Upper Bounds on REE Rates

This section first introduces notions required for establishing upper bounds on REE rates, including enode graphs, REE procedures, and the number of established EQPs under certainty equivalence (CE). Then the upper bounds are presented.

A. Enode Graphs and REE Procedures

Enodes and enode graphs are notions used for describing quantum operations performed on a chain. In particular,

an enode corresponds to entanglement established between two nodes in the quantum network. The definition of an enode is presented in the following.

Definition 1 (Enode): Let i and j represent two nodes on the chain with $i < j$. An enode $\mathrm{e}_c^{i,j}$ represents qubit pairs between nodes i and j, where $c \in \mathbb{N}$ specifies the rounds of distillations that have been performed between nodes i and j after link (i, j) is created. □

For example, $\mathrm{e}_0^{0,1}$ represents CQPs between nodes 0 and 1 obtained via entanglement generation, $\mathrm{e}_1^{0,1}$ represents qubit pairs between nodes 0 and 1 obtained by performing one round of distillation on CQPs between these two nodes, whereas $\mathrm{e}_0^{0,2}$ represents qubit pairs between nodes 0 and 2 obtained by performing swapping between nodes 0 and 2 at node 1.

An enode graph is a directed acyclic graph (DAG) [80]. In a DAG, if there is an edge pointing from vertex v_1 to vertex v_2, then v_1 is called a predecessor of v_2 and v_2 is called a successor of v_1. Let l_1 and l_2 be the indices of two nodes on the chain with $0 \leqslant l_1 < l_2 \leqslant L$. Then $l_1 : l_2$ represents a chain with l_1 and l_2 being the source node and destination node, respectively. An enode graph for $l_1 : l_2$ is defined below.[1]

Definition 2 (Enode Graph): An enode graph $\mathcal{G}_\mathrm{e}$ for a chain $l_1 : l_2$ is a DAG that satisfies the following conditions.

- Each vertex of $\mathcal{G}_\mathrm{e}$ is an enode $\mathrm{e}_c^{i,j}$ with $l_1 \leqslant i < j \leqslant l_2$.
- Graph $\mathcal{G}_\mathrm{e}$ has $l_2 - l_1$ vertices with zero predecessor. These vertices are $\mathrm{e}_0^{l_1,l_1+1}, \mathrm{e}_0^{l_1+1,l_1+2}, \ldots, \mathrm{e}_0^{l_2-1,l_2}$ representing CQPs generated over elementary links.
- Graph $\mathcal{G}_\mathrm{e}$ has one vertex with zero successor. This vertex is $\mathrm{e}_c^{l_1,l_2}$ for some $c \in \mathbb{N}$ representing established qubit pairs between nodes l_1 and l_2. Each of the other vertices has one successor.
- There is an edge pointing from $\mathrm{e}_c^{i,j}$ to $\mathrm{e}_{c+1}^{i,j}$ if entanglement distillation $\mathrm{d}^{i,j}$ is performed consuming qubit pairs represented by $\mathrm{e}_c^{i,j}$.
- There is an edge pointing from $\mathrm{e}_{c_1}^{i,j}$ to $\mathrm{e}_0^{i,l}$ and an edge pointing from $\mathrm{e}_{c_2}^{j,l}$ to $\mathrm{e}_0^{i,l}$ if entanglement swapping $\mathrm{s}^{i,j,l}$ is performed consuming qubit pairs represented by $\mathrm{e}_{c_1}^{i,j}$ and $\mathrm{e}_{c_2}^{j,l}$ for $c_1 \in \mathbb{N}$ and $c_2 \in \mathbb{N}$. □

By definition, except for vertices with zero predecessor, all the vertices have either one or two predecessors. If $\mathrm{e}_0^{i,l}$ has two predecessors $\mathrm{e}_{c_1}^{i,j}$ and $\mathrm{e}_{c_2}^{j,l}$ with $i < j < l$, then $\mathrm{e}_{c_1}^{i,j}$ and $\mathrm{e}_{c_2}^{j,l}$ are referred to as the left predecessor and right predecessor, respectively, of $\mathrm{e}_0^{i,l}$. Two examples of enode graphs on a chain $0 : 2$ are shown in Fig. 2. The enodes and enode graphs defined in this paper are generalizations of those introduced in [37]. Specifically, these two notions reduce to those defined in [37] if entanglement distillation is not considered.

Given an enode graph $\mathcal{G}_\mathrm{e}$ and a vertex v on $\mathcal{G}_\mathrm{e}$, define $\mathcal{G}(v)$ as a subgraph of $\mathcal{G}_\mathrm{e}$ consisting of all the vertices that can reach v as well as the edges between these vertices. Here, vertex v' can reach vertex v if there is a path that starts at v' and ends at v. In particular, any vertex v reaches itself. An example of such a subgraph is shown in Fig. 2(a).

[1]Employing enode graphs for the design of REE policies is akin to the philosophy of solving difficult problems in the transform domain [81], [82]. This philosophy has been applied to address both classical and quantum communication problems [37], [83], [84].

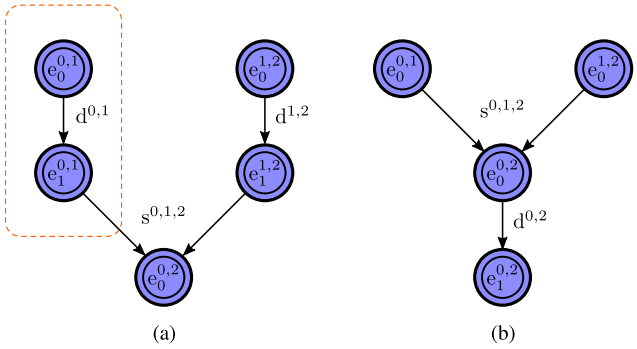

Fig. 2. Enode graphs on a chain $0 : 2$. (a): enode graph associated with REE procedure $\boldsymbol{u}_\mathrm{a} := (\mathrm{d}^{0,1}, \mathrm{d}^{1,2}, \mathrm{s}^{0,1,2})$. Subgraph $\mathcal{G}(\mathrm{e}_1^{0,1})$ contains nodes inside the orange dashed rectangle. (b): enode graph associated with REE procedure $\boldsymbol{u}_\mathrm{b} := (\mathrm{s}^{0,1,2}, \mathrm{d}^{0,2})$. Entanglement distillation corresponding to vertical arrows and entanglement swapping corresponding to slanted arrows are also shown.

An REE procedure is a sequence of entanglement distillation and swapping operations. To present the notion of REE procedures, we define a sequence of quantum operations associated with an enode graph as follows.

Definition 3: Let v represent the vertex in an enode graph $\mathcal{G}_\mathrm{e}$ for a chain $l_1 : l_2$ with zero successor. Define a sequence $\boldsymbol{h}(\mathcal{G}_\mathrm{e})$ as follows.

- If v is the only node in $\mathcal{G}_\mathrm{e}$, then $\boldsymbol{h}(\mathcal{G}_\mathrm{e})$ is an empty sequence.
- If v has only one predecessor $\mathrm{e}_c^{i,j}$ with $c \in \mathbb{N}$, then

$$\boldsymbol{h}(\mathcal{G}_\mathrm{e}) = \left(\boldsymbol{h}\left(\mathcal{G}\left(\mathrm{e}_c^{i,j}\right)\right), \mathrm{d}^{i,j}\right).$$

- If v has a left predecessor $\mathrm{e}_{c_1}^{i,j}$ and a right predecessor $\mathrm{e}_{c_2}^{j,l}$ with $c_1, c_2 \in \mathbb{N}$, then

$$\boldsymbol{h}(\mathcal{G}_\mathrm{e}) = \left(\boldsymbol{h}\left(\mathcal{G}\left(\mathrm{e}_{c_1}^{i,j}\right)\right), \boldsymbol{h}\left(\mathcal{G}\left(\mathrm{e}_{c_2}^{j,l}\right)\right), \mathrm{s}^{i,j,l}\right). \quad (7)$$

□

REE procedures are defined in the following.

Definition 4 (REE Procedure): A sequence $\boldsymbol{u}$ is an REE procedure if $\boldsymbol{u} = \boldsymbol{h}(\mathcal{G}_\mathrm{e})$ for some enode graph $\mathcal{G}_\mathrm{e}$. In particular, $\boldsymbol{u}$ is referred to as an REE procedure associated with $\mathcal{G}_\mathrm{e}$. □

As an example, the REE procedures associated with enode graphs shown in Fig. 2 are presented in the caption of that figure. For simplicity, an REE procedure associated with an enode graph on chain $l_1 : l_2$ is referred to as an REE procedure on $l_1 : l_2$. Recall that an REE policy involves selecting different REE procedures, allocating a proportion of the CQP budget to each selected REE procedure, generating CQPs according to the allocated budget, and consuming these CQPs to perform the quantum operations according to the selected REE procedure.

Remark 1: In the case corresponding to the third bullet of Definition 3, the quantum operations associated with $\mathcal{G}\left(\mathrm{e}_{c_1}^{i,j}\right)$ containing the left predecessor $\mathrm{e}_{c_1}^{i,j}$ are arranged in front of quantum operations associated with $\mathcal{G}\left(\mathrm{e}_{c_2}^{j,l}\right)$ containing the right predecessor $\mathrm{e}_{c_2}^{j,l}$, as shown in (7). The following two comments are made on such an arrangement. First, this arrangement is chosen to ensure that there is only one sequence of quantum operations associated with an enode graph. For example, if an alternative arrangement is adopted so that

quantum operations associated with $\mathcal{G}(\mathrm{e}_{c_2}^{j,l})$ are in front of those associated with $\mathcal{G}(\mathrm{e}_{c_1}^{i,j})$, i.e., $\boldsymbol{h}(\mathcal{G}(\mathrm{e}_{c_1}^{i,j}))$ and $\boldsymbol{h}(\mathcal{G}(\mathrm{e}_{c_2}^{j,l}))$ in (7) are switched, then a different sequence of quantum operations associated with the same enode graph would be defined. Employing the arrangement in Definition 3 avoids such a sequence and thus simplifies the presentation of the paper. Second, this arrangement is unrelated to the order in which quantum operations associated with $\mathcal{G}(\mathrm{e}_{c_1}^{i,j})$ and $\mathcal{G}(\mathrm{e}_{c_2}^{j,l})$ are performed in practice. Indeed, quantum operations associated with $\mathcal{G}(\mathrm{e}_{c_2}^{j,l})$ can be performed in parallel with or before those associated with $\mathcal{G}(\mathrm{e}_{c_1}^{i,j})$. □

An REE procedure $\boldsymbol{u}$ on a chain $l_1 : l_2$ has the following properties. First, if the length of the chain $l_2 - l_1$ equals 1, then $\boldsymbol{u} = \mathbf{d}_c^{l_1,l_2}$ for some $c \in \mathbb{N}$. Second, if $l_2 - l_1 > 1$, then $\boldsymbol{u}$ can be written as

$$\boldsymbol{u} = \left(\boldsymbol{u}_{\mathrm{L}},\, \boldsymbol{u}_{\mathrm{R}},\, \mathrm{s}^{l_1,l,l_2},\, \mathbf{d}_c^{l_1,l_2}\right) \tag{8}$$

where l is a node index satisfying $l_1 < l < l_2$, sequences $\boldsymbol{u}_{\mathrm{L}}$ and $\boldsymbol{u}_{\mathrm{R}}$ represent REE procedures on $l_1 : l$ and $l : l_2$, respectively, and $c \in \mathbb{N}$. For example, $\boldsymbol{u}_{\mathrm{a}}$ associated with Fig. 2(a) can be written as in (8) with $\boldsymbol{u}_{\mathrm{L}} = \mathrm{d}^{0,1}$, $\boldsymbol{u}_{\mathrm{R}} = \mathrm{d}^{1,2}$, $l = 1$, and $c = 0$; REE procedure $\boldsymbol{u}_{\mathrm{b}}$ associated with Fig. 2(b) can be written as in (8) with $\boldsymbol{u}_{\mathrm{L}}$ and $\boldsymbol{u}_{\mathrm{R}}$ being empty sequences, $l = 1$, and $c = 1$. Note that the subscripts 'L' and 'R' indicate that $l_1 : l$ and $l : l_2$ can be viewed as a left sub-chain and a right sub-chain, respectively, of $l_1 : l_2$. The connection between (8) and enode graph is explained in the following. Let $\mathcal{G}_{\mathrm{e}}$ be the enode graph that $\boldsymbol{u}$ is associated with, i.e., $\boldsymbol{u} = \boldsymbol{h}(\mathcal{G}_{\mathrm{e}})$. Then $\mathcal{G}_{\mathrm{e}}$ contains a vertex $\mathrm{e}_0^{l_1,l_2}$ whose left predecessor and right predecessor are $\mathrm{e}_{c_1}^{l_1,l}$ and $\mathrm{e}_{c_2}^{l,l_2}$, respectively, for some $c_1, c_2 \in \mathbb{N}$. In particular, $\mathrm{e}_0^{l_1,l_2}$ represents qubit pairs obtained via entanglement swapping s^{l_1,l,l_2}. REE procedure $\boldsymbol{u}$ can be written as in (8), where $\boldsymbol{u}_{\mathrm{L}}$ and $\boldsymbol{u}_{\mathrm{R}}$ are associated with subgraphs $\mathcal{G}(\mathrm{e}_{c_1}^{l_1,l})$ and $\mathcal{G}(\mathrm{e}_{c_2}^{l,l_2})$, respectively, i.e., $\boldsymbol{u}_{\mathrm{L}} = \boldsymbol{h}(\mathcal{G}(\mathrm{e}_{c_1}^{l_1,l}))$ and $\boldsymbol{u}_{\mathrm{R}} = \boldsymbol{h}(\mathcal{G}(\mathrm{e}_{c_2}^{l,l_2}))$.

Using CQPs generated over elementary links on a chain $l_1 : l_2$, EQPs between nodes l_1 and l_2 can be established by performing in sequence the quantum operations that make up an REE procedure $\boldsymbol{u}$. This procedure is called "performing $\boldsymbol{u}$ on the chain." The fidelity of the established qubit pairs is affected by the fidelities of CQPs consumed performing $\boldsymbol{u}$. To explain this, define the *CQP fidelity vector* $\boldsymbol{w}$ for chain $l_1 : l_2$ as

$$\boldsymbol{w} := \begin{bmatrix} w^{l_1,l_1+1} & w^{l_1+1,l_1+2} & \cdots & w^{l_2-1,l_2} \end{bmatrix}^{\mathrm{T}} \tag{9}$$

where $w^{l-1,l}$ represents the fidelity of CQPs between nodes $l-1$ and l before $\boldsymbol{u}$ is performed for $l = l_1+1, l_1+2, \ldots, l_2$. Note that $\boldsymbol{w}$ defined in (5b) is a special case of definition (9) with $l_1 = 0$ and $l_2 = L$. The fidelity of qubit pairs successfully established between nodes l_1 and l_2 after performing $\boldsymbol{u}$ is a deterministic function $g_{\boldsymbol{u}}(\boldsymbol{w})$ of $\boldsymbol{w}$ parameterized by $\boldsymbol{u}$. This function is a composition of $g_{\mathrm{s}}(\cdot,\cdot)$ and $g_{\mathrm{d}}(\cdot)$ given by (4) and (3) and is obtained in a recursive manner. For the case where the length of the chain $l_2 - l_1$ is 1, it holds that $\boldsymbol{u} = \mathbf{d}_c^{l_1,l_2}$ for some $c \in \mathbb{N}$, and $g_{\boldsymbol{u}}(\boldsymbol{w}) = g_{\mathrm{d}}^{\circ c}(w^{l_1,l_2})$. For the case where $l_2 - l_1 > 1$, write $\boldsymbol{u}$ as in (8), and partition $\boldsymbol{w}$ as $\boldsymbol{w} = \begin{bmatrix} \boldsymbol{w}_{\mathrm{L}}^{\mathrm{T}} & \boldsymbol{w}_{\mathrm{R}}^{\mathrm{T}} \end{bmatrix}^{\mathrm{T}}$, where

$$\boldsymbol{w}_{\mathrm{L}} := [\boldsymbol{w}]_{1:l-l_1} \quad \boldsymbol{w}_{\mathrm{R}} := [\boldsymbol{w}]_{l-l_1+1:l_2-l_1}\,. \tag{10}$$

Then $g_{\boldsymbol{u}}(\boldsymbol{w})$ is given by

$$g_{\boldsymbol{u}}(\boldsymbol{w}) = g_{\mathrm{d}}^{\circ c}\Big(g_{\mathrm{s}}\big(g_{\boldsymbol{u}_{\mathrm{L}}}(\boldsymbol{w}_{\mathrm{L}}),\, g_{\boldsymbol{u}_{\mathrm{R}}}(\boldsymbol{w}_{\mathrm{R}})\big)\Big)\,.$$

As an example, for $\boldsymbol{u}_{\mathrm{a}}$ and $\boldsymbol{u}_{\mathrm{b}}$ shown in Fig. 2, $g_{\boldsymbol{u}_{\mathrm{a}}}(\boldsymbol{w}) = g_{\mathrm{s}}\big(g_{\mathrm{d}}(w^{0,1}),\, g_{\mathrm{d}}(w^{1,2})\big)$ and $g_{\boldsymbol{u}_{\mathrm{b}}}(\boldsymbol{w}) = g_{\mathrm{d}}\big(g_{\mathrm{s}}(w^{0,1},\, w^{1,2})\big)$.

Building on the definition of $g_{\boldsymbol{u}}(\boldsymbol{w})$, we define feasible REE procedures as follows.

Definition 5 (Feasible REE Procedure): An REE procedure $\boldsymbol{u}$ on a chain is said to be feasible for CQP fidelity vector $\boldsymbol{w}$ and EQP fidelity threshold $\underline{w}$ if the fidelity of qubit pairs established by performing $\boldsymbol{u}$ exceeds $\underline{w}$, i.e., $g_{\boldsymbol{u}}(\boldsymbol{w}) > \underline{w}$. □

The number of qubit pairs established by performing an REE procedure is a random variable and is affected by the fidelities and number of CQPs consumed by this REE procedure. To formalize this concept, define the *CQP number vector* $\boldsymbol{n}$ for chain $l_1 : l_2$ as

$$\boldsymbol{n} := \begin{bmatrix} n^{l_1,l_1+1} & n^{l_1+1,l_1+2} & \cdots & n^{l_2-1,l_2} \end{bmatrix}^{\mathrm{T}}$$

where $n^{l-1,l}$ represents the number of CQPs between nodes $l-1$ and l before $\boldsymbol{u}$ is performed. The number of qubit pairs established between nodes l_1 and l_2 after performing $\boldsymbol{u}$ is a random variable and is denoted by $\check{\mathrm{z}}_{\boldsymbol{u}}(\boldsymbol{n}, \boldsymbol{w})$.

The distribution of $\check{\mathrm{z}}_{\boldsymbol{u}}(\boldsymbol{n}, \boldsymbol{w})$ is obtained in a recursive manner. For the case where the length of the chain $l_2 - l_1$ is 1, it holds that $\boldsymbol{u} = \mathbf{d}_c^{l_1,l_2}$ for some $c \in \mathbb{N}$, and

$$\check{\mathrm{z}}_{\boldsymbol{u}}(\boldsymbol{n}, \boldsymbol{w}) \sim \mathrm{Bin}\Big(\Big\lfloor \frac{n^{l_1,l_2}}{2^c} \Big\rfloor,\, \prod_{k=1}^{c} p_{\mathrm{d}}\big(g_{\mathrm{d}}^{\circ(k-1)}(w^{l_1,l_2})\big)\Big). \tag{11}$$

To explain (11), note that obtaining one qubit pair via c rounds of distillation requires 2^c CQPs, and all the c rounds of distillation need to be successful. In particular, since the fidelity of qubit pairs before the kth round of distillation is $g_{\mathrm{d}}^{\circ(k-1)}(w^{l_1,l_2})$, the success probability of the kth round of distillation is $p_{\mathrm{d}}\big(g_{\mathrm{d}}^{\circ(k-1)}(w^{l_1,l_2})\big)$. Consequently, the probability that all the c rounds of distillation are successful is the second parameter of the binomial distribution in (11). Note that the product in (11), i.e., the success probability of the binomial distribution, must be interpreted as 1 if $c = 0$.

For the case where $l_2 - l_1 > 1$, write $\boldsymbol{u}$ as in (8), and partition $\boldsymbol{n}$ as $\boldsymbol{n} = \begin{bmatrix} \boldsymbol{n}_{\mathrm{L}}^{\mathrm{T}} & \boldsymbol{n}_{\mathrm{R}}^{\mathrm{T}} \end{bmatrix}^{\mathrm{T}}$, where

$$\boldsymbol{n}_{\mathrm{L}} := [\boldsymbol{n}]_{1:l-l_1} \quad \text{and} \quad \boldsymbol{n}_{\mathrm{R}} := [\boldsymbol{n}]_{l-l_1+1:l_2-l_1}\,. \tag{12}$$

To derive the distribution of $\check{\mathrm{z}}_{\boldsymbol{u}}(\boldsymbol{n}, \boldsymbol{w})$, consider the number of qubit pairs $\check{\mathrm{z}}_{\breve{\boldsymbol{u}}}(\boldsymbol{n}, \boldsymbol{w})$ after performing $\breve{\boldsymbol{u}}$ defined as

$$\breve{\boldsymbol{u}} := \left(\boldsymbol{u}_{\mathrm{L}}, \boldsymbol{u}_{\mathrm{R}}, \mathrm{s}^{l_1,l,l_2}\right). \tag{13}$$

Note that $\boldsymbol{u} = \left(\breve{\boldsymbol{u}}, \mathbf{d}_c^{l_1,l_2}\right)$ according to (8). By definition, the number of qubit pairs on $l_1 : l$ and on $l : l_2$ immediately before performing s^{l_1,l,l_2} are $\check{\mathrm{z}}_{\boldsymbol{u}_{\mathrm{L}}}(\boldsymbol{n}_{\mathrm{L}})$ and $\check{\mathrm{z}}_{\boldsymbol{u}_{\mathrm{R}}}(\boldsymbol{n}_{\mathrm{R}})$, respectively. After performing s^{l_1,l,l_2}, the number of qubit pairs between nodes l_1 and l_2 becomes $\check{\mathrm{z}}_{\breve{\boldsymbol{u}}}(\boldsymbol{n}, \boldsymbol{w})$, which satisfies

$$\check{\mathrm{z}}_{\breve{\boldsymbol{u}}}(\boldsymbol{n}, \boldsymbol{w}) \sim \mathrm{Bin}\big(\min\big\{\check{\mathrm{z}}_{\boldsymbol{u}_{\mathrm{L}}}(\boldsymbol{n}_{\mathrm{L}}), \check{\mathrm{z}}_{\boldsymbol{u}_{\mathrm{R}}}(\boldsymbol{n}_{\mathrm{R}})\big\}, q\big). \tag{14}$$

Finally, $\mathbf{d}_c^{l_1,l_2}$ is performed consuming these $\check{\mathsf{z}}_{\check{\boldsymbol{u}}}(\boldsymbol{n},\boldsymbol{w})$ qubit pairs in order to complete performing $\boldsymbol{u}$. Consequently, for $l_2-l_1>1$,

$$\check{\mathsf{z}}_{\boldsymbol{u}}(\boldsymbol{n},\boldsymbol{w}) \sim \mathrm{Bin}\Big(\Big\lfloor \frac{\check{\mathsf{z}}_{\check{\boldsymbol{u}}}(\boldsymbol{n},\boldsymbol{w})}{2^c} \Big\rfloor, \prod_{k=1}^{c} p_{\mathrm{d}}\big(g_{\mathrm{d}}^{\circ(k-1)}(w^{l_1,l_2})\big)\Big). \tag{15}$$

Using the notion of REE procedures, an REE policy π on a chain $l_1:l_2$ can be decomposed into multiple iterations, where each iteration consists of: 1) generating CQPs over each elementary link using a proportion of the budget, and 2) establishing EQPs by performing a feasible REE procedure consuming the generated CQPs. Then the REE rate of π is the total expected number of established EQPs in all iterations divided by the average budget. Specifically, let $n_k^{l-1,l}$ represent the number of CQPs generated between nodes $l-1$ and l in the kth iteration, and define the generation vector of the kth iteration as $\boldsymbol{n}_k := \begin{bmatrix} n_k^{l_1,l_1+1} & n_k^{l_1+1,l_1+2} & \cdots & n_k^{l_2-1,l_2}\end{bmatrix}^{\mathrm{T}}$. The total number of allocated CQPs of all the iterations over each elementary link cannot exceed its budget. That is, $\sum_k \boldsymbol{n}_k \preccurlyeq \boldsymbol{b}$, where $\boldsymbol{b} := \begin{bmatrix} b^{l_1,l_1+1} & b^{l_1+1,l_1+2} & \cdots & b^{l_2-1,l_2}\end{bmatrix}^{\mathrm{T}}$ represents the CQP budget vector. Denote the REE procedure performed in the kth iteration by $\boldsymbol{u}_k$. Then the expected number of established EQPs in the kth iteration is $\mathbb{E}\{\check{\mathsf{z}}_{\boldsymbol{u}_k}(\boldsymbol{n}_k,\boldsymbol{w})\}$. Consequently, the REE rate $r_\pi(\boldsymbol{b},\boldsymbol{w})$ of this policy is given by

$$r_\pi(\boldsymbol{b},\boldsymbol{w}) = \frac{l_2-l_1}{|\boldsymbol{b}|}\sum_{k=1}^{K}\mathbb{E}\{\check{\mathsf{z}}_{\boldsymbol{u}_k}(\boldsymbol{n}_k,\boldsymbol{w})\} \tag{16}$$

where K represents the total number of iterations. This shows that determining the optimal policy is equivalent to determining the total number K of iterations, the generation vector $\boldsymbol{n}_k$, and the REE procedure $\boldsymbol{u}_k$ performed in each iteration $k=1,2,\ldots,K$.

B. Number of Established EQPs Under Certainty Equivalence

The number of EQPs established by an REE under CE is a notion motivated as follows. Computing the expected number of established EQPs $\mathbb{E}\{\check{\mathsf{z}}_{\boldsymbol{u}}(\boldsymbol{n},\boldsymbol{w})\}$ is challenging in general, making optimal REE policies difficult to design. One method for obtaining insights into the design of REE policies is to approximate the expected number of established EQPs via a technique named CE. This technique replaces random variables by their expected values, thereby removing randomness and simplifying mathematical calculations. CE is a technique that has been applied in control theory and reinforcement learning [85], [86], [87]. For example, it was shown that applying CE does not affect the optimal control policies for linear-quadratic-Gaussian (LQG) control problems [88], [89], [90]. In LQG control problems, the aim is to design control signal for each instant of time in order to stabilize the states of a linear system perturbed by process noise that follows a Gaussian distribution. The control signal is a function of linear observations of the states in the presence of measurement noise that follows a Gaussian distribution. The objective is to minimize a quadratic function of the states and control signals. LQG problems can be solved via CE, where the optimal control law treats the conditional expectation of the state given the observations as the true state value. LQG problems are completely different than the REE problem studied in this paper: in the REE problem, the status of the quantum repeater chain cannot be modeled as a linear system, the objective function is not quadratic, and the randomness of the system is due to the failure of entanglement distillation and swapping instead of process noise and measurement noise.

To explain approximation via CE, consider calculating $\mathbb{E}\{\check{\mathsf{z}}_{\boldsymbol{u}}(\boldsymbol{n},\boldsymbol{w})\}$ for an REE procedure $\boldsymbol{u}$ that can be written as in (8). Using the law of iterated expectations [91],

$$\mathbb{E}\{\check{\mathsf{z}}_{\boldsymbol{u}}(\boldsymbol{n},\boldsymbol{w})\} = \mathbb{E}\Big\{\mathbb{E}\{\check{\mathsf{z}}_{\boldsymbol{u}}(\boldsymbol{n},\boldsymbol{w}) \,\big|\, \check{\mathsf{z}}_{\check{\boldsymbol{u}}}(\boldsymbol{n},\boldsymbol{w})\}\Big\} \tag{17}$$

where $\check{\boldsymbol{u}}$ is defined in (13). The conditional distribution of $\check{\mathsf{z}}_{\boldsymbol{u}}(\boldsymbol{n},\boldsymbol{w})$ given $\check{\mathsf{z}}_{\check{\boldsymbol{u}}}(\boldsymbol{n},\boldsymbol{w})$ is shown in (15). Omitting the floor function in (15), we can approximate the conditional expectation in (17) by $\check{\mathsf{z}}_{\check{\boldsymbol{u}}}(\boldsymbol{n},\boldsymbol{w})\beta(c,w^{l_1,l_2})$, where the function $\beta(\cdot,\cdot)$ is defined as

$$\beta(m,w) := \frac{1}{2^m}\prod_{k=1}^{m} p_{\mathrm{d}}\big(g_{\mathrm{d}}^{\circ(k-1)}(w)\big) \qquad m\in\mathbb{N},\quad 1/2<w\leqslant 1. \tag{18}$$

Note that $\beta(\cdot,\cdot)$ is the inverse of the notion "purification resources" defined in [61]. Substituting this approximate conditional expectation into (17), $\mathbb{E}\{\check{\mathsf{z}}_{\boldsymbol{u}}(\boldsymbol{n},\boldsymbol{w})\}$ is approximated by $\mathbb{E}\{\check{\mathsf{z}}_{\check{\boldsymbol{u}}}(\boldsymbol{n},\boldsymbol{w})\}\beta(c,w^{l_1,l_2})$. Applying (14),

$$\mathbb{E}\{\check{\mathsf{z}}_{\check{\boldsymbol{u}}}(\boldsymbol{n},\boldsymbol{w})\} = q\,\mathbb{E}\Big\{\min\big\{\check{\mathsf{z}}_{\boldsymbol{u}_{\mathrm{L}}}(\boldsymbol{n}_{\mathrm{L}}),\,\check{\mathsf{z}}_{\boldsymbol{u}_{\mathrm{R}}}(\boldsymbol{n}_{\mathrm{R}})\big\}\Big\}. \tag{19}$$

Applying CE, we approximate $\check{\mathsf{z}}_{\boldsymbol{u}_{\mathrm{L}}}(\boldsymbol{n}_{\mathrm{L}})$ and $\check{\mathsf{z}}_{\boldsymbol{u}_{\mathrm{R}}}(\boldsymbol{n}_{\mathrm{R}})$ by their expectations. As a result, $\mathbb{E}\{\check{\mathsf{z}}_{\boldsymbol{u}}(\boldsymbol{n},\boldsymbol{w})\}$ is approximated by

$$q\min\big\{\mathbb{E}\{\check{\mathsf{z}}_{\boldsymbol{u}_{\mathrm{L}}}(\boldsymbol{n}_{\mathrm{L}})\},\,\mathbb{E}\{\check{\mathsf{z}}_{\boldsymbol{u}_{\mathrm{R}}}(\boldsymbol{n}_{\mathrm{R}})\}\big\}\,\beta\big(c,w^{l_1,l_2}\big).$$

The above procedure can be used for approximating $\mathbb{E}\{\check{\mathsf{z}}_{\boldsymbol{u}_{\mathrm{L}}}(\boldsymbol{n}_{\mathrm{L}})\}$ and $\mathbb{E}\{\check{\mathsf{z}}_{\boldsymbol{u}_{\mathrm{R}}}(\boldsymbol{n}_{\mathrm{R}})\}$. As a result, an approximation of $\mathbb{E}\{\check{\mathsf{z}}_{\boldsymbol{u}}(\boldsymbol{n},\boldsymbol{w})\}$ is obtained via CE in a recursive manner.

Using the above idea, the number of EQPs established by an REE procedure under CE is defined as follows.

Definition 6 (Number of Established EQPs Under CE): Let $\boldsymbol{n}$ and $\boldsymbol{w}$ represent a CQP number vector and a CQP fidelity vector, respectively, on chain $l_1:l_2$, and let $\boldsymbol{u}$ represent an REE procedure on this chain. The number $\zeta_{\boldsymbol{u}}(\boldsymbol{n},\boldsymbol{w})$ of EQPs established by $\boldsymbol{u}$ under CE is defined as follows.

- If $l_2-l_1=1$, then $\boldsymbol{u}=\mathbf{d}_c^{l_1,l_2}$ for some $c\in\mathbb{N}$. In this case,
$$\zeta_{\boldsymbol{u}}(\boldsymbol{n},\boldsymbol{w}) := \beta\big(c,w^{l_1,l_2}\big)\,n^{l_1,l_2}. \tag{20}$$
- If $l_2-l_1>1$, then $\boldsymbol{u}$ can be written as in (8). In this case,
$$\zeta_{\boldsymbol{u}}(\boldsymbol{n},\boldsymbol{w}) := q\min\big\{\zeta_{\boldsymbol{u}_{\mathrm{L}}}(\boldsymbol{n}_{\mathrm{L}},\boldsymbol{w}_{\mathrm{L}}),\,\zeta_{\boldsymbol{u}_{\mathrm{R}}}(\boldsymbol{n}_{\mathrm{R}},\boldsymbol{w}_{\mathrm{R}})\big\} \times\beta\big(c,g_{\check{\boldsymbol{u}}}(\boldsymbol{w})\big) \tag{21}$$
where $\boldsymbol{n}_{\mathrm{L}}$, $\boldsymbol{w}_{\mathrm{L}}$, $\boldsymbol{n}_{\mathrm{R}}$, and $\boldsymbol{w}_{\mathrm{R}}$ are defined in (10) and (12), while $\check{\boldsymbol{u}}$ is defined in (13).

□

Remark 2: It should be emphasized that the upper bound (25) to be established in this section is on the exact optimal REE rate $r^*(\boldsymbol{b},\boldsymbol{w})$, which is calculated without any approximation. Indeed, the approximation via CE aims only to provide insights into the design of REE policies and to serve as a tool for proving the upper bound. Note that by law of large numbers, the accuracy of approximation via CE is improved when the number of CQPs generated over each elementary link becomes sufficiently large. □

The next proposition shows properties of $\zeta_{\boldsymbol{u}}(\boldsymbol{n},\boldsymbol{w})$ that will be used later.

Proposition 1: Function $\zeta_{\boldsymbol{u}}(\boldsymbol{n},\boldsymbol{w})$ has the following properties.

1) Monotonicity: if $\boldsymbol{n}\succcurlyeq\boldsymbol{n}'$, then $\zeta_{\boldsymbol{u}}(\boldsymbol{n},\boldsymbol{w})\geqslant\zeta_{\boldsymbol{u}}(\boldsymbol{n}',\boldsymbol{w})$.
2) Concavity: $\zeta_{\boldsymbol{u}}(\boldsymbol{n},\boldsymbol{w})$ is concave with respect to $\boldsymbol{n}$.
3) Upper bound on expected number of established EQPs: the following inequality holds for arbitrary $\boldsymbol{n}$ and $\boldsymbol{w}$

$$\mathbb{E}\big\{\check{\mathrm{z}}_{\boldsymbol{u}}(\boldsymbol{n},\boldsymbol{w})\big\}\leqslant\zeta_{\boldsymbol{u}}(\boldsymbol{n},\boldsymbol{w})\,. \tag{22}$$

□

Proof: The proposition can be proved via induction. In particular, Jensen's inequality is used for proving the third property. Details of the proof are omitted. ⊠

Finally, the notion of efficient REE procedures under CE is introduced.

Definition 7: Let $\boldsymbol{w}$ represent a CQP fidelity vector on a chain and let $\underline{w}$ represent an EQP fidelity threshold. Moreover, let $\boldsymbol{u}$ represent a feasible REE procedure for $\boldsymbol{w}$ and $\underline{w}$ on this chain. Procedure $\boldsymbol{u}$ is said to be efficient for $\boldsymbol{w}$ and $\underline{w}$ under CE if there does not exist a different feasible REE procedure $\boldsymbol{u}'$ on this chain such that $\zeta_{\boldsymbol{u}}(\boldsymbol{n},\boldsymbol{w})\leqslant\zeta_{\boldsymbol{u}'}(\boldsymbol{n},\boldsymbol{w})$ for all $\boldsymbol{n}\succcurlyeq\boldsymbol{0}$. □

C. REE Procedures of Class $\mathcal{D}$

This subsection introduces one type of REE procedures named procedures of class $\mathcal{D}$. This type of REE procedures will be used in the proof of the upper bound and in the construction of an REE policy that achieves this bound asymptotically when the budget of CQPs for each elementary link becomes sufficiently large. REE procedures of class $\mathcal{D}$ are defined as follows.

Definition 8: An REE procedure on chain $l_1:l_2$ is of class $\mathcal{D}$ if all the distillation operations are performed only between nodes $l-1$ and l for $l=l_1+1,l_1+2,\ldots,l_2$. □

Distillation between nodes $l-1$ and l is referred to as distillation over the elementary link $(l-1,l)$. In an REE procedure of class $\mathcal{D}$, distillation operations are performed over elementary links before these links are destroyed by swapping operations for creating longer links. For example, procedure $\boldsymbol{u}_{\mathrm{a}}$ shown in Fig. 2(a) is of class $\mathcal{D}$, where distillation is performed between nodes 0 and 1 as well as between nodes 1 and 2 before swapping $\mathrm{s}^{0,1,2}$ is performed. On the other hand, $\boldsymbol{u}_{\mathrm{b}}$ in Fig. 2(b) is not of class $\mathcal{D}$, since distillation $\mathrm{d}^{0,2}$ is performed over $(0,2)$, which is not an elementary link.

The next proposition shows the significance of REE procedures of class $\mathcal{D}$.

Proposition 2: All the REE procedures that are efficient under CE (see Definition 7) are of class $\mathcal{D}$. □

Proof: The proposition is proved by showing that given a feasible REE procedure $\boldsymbol{u}$, an REE procedure $\boldsymbol{u}'$ of class $\mathcal{D}$ can be constructed such that the fidelity of the EQPs established by $\boldsymbol{u}'$ and the number of the EQPs established by $\boldsymbol{u}'$ under CE are no smaller than those established by $\boldsymbol{u}$. See Appendix A for details. ⊠

Remark 3: Proposition 2 shows the advantage of REE procedures of class $\mathcal{D}$ in terms of the number of established EQPs under CE. The proposition exploits CE to alleviate the need for the exact value of the expected number of established EQPs. □

Next, the notion of allocation vector for an REE procedure of class $\mathcal{D}$ is introduced. An allocation vector for an REE procedure $\boldsymbol{u}$ on chain $l_1:l_2$ is an (l_2-l_1)-dimensional real vector. This vector specifies the number of CQPs that should be generated under CE over each elementary link for establishing one qubit pair between l_1 and l_2 if $\boldsymbol{u}$ is performed. In particular, the lth entry of this allocation vector indicates the number of CQPs that should be generated over (l_1+l-1,l_1+l) for $l=1,2,\ldots,l_2-l_1$. An allocation vector can be determined by calculating the number of qubit pairs needed at each enode of the enode graph associated with the REE procedure. Such calculation is conducted from the bottom of the enode graph to its top. As an example, consider the allocation vector for REE procedure $\boldsymbol{u}_{\mathrm{a}}$ shown in Fig. 2(a). In order to obtain one qubit pair between nodes 0 and 2 at enode $\mathrm{e}_0^{0,2}$, $1/q$ qubit pairs would be needed at enodes $\mathrm{e}_1^{0,1}$ and $\mathrm{e}_1^{1,2}$ before the swapping $\mathrm{s}^{0,1,2}$ is performed, since the success probability of swapping is q. To obtain $1/q$ qubit pairs at enode $\mathrm{e}_1^{0,1}$, a total number of $2/(qp_{\mathrm{d}}(w^{0,1}))$ qubit pairs are needed at enode $\mathrm{e}_0^{0,1}$ before the distillation $\mathrm{d}^{0,1}$ is performed, since two qubit pairs are consumed for obtaining one distilled qubit pair with success probability $p_{\mathrm{d}}(w^{0,1})$. Similarly, $2/(qp_{\mathrm{d}}(w^{1,2}))$ qubit pairs are needed at enode $\mathrm{e}_0^{1,2}$. Consequently, the allocation vector for $\boldsymbol{u}_{\mathrm{a}}$ is $\big[2/(qp_{\mathrm{d}}(w^{0,1}))\quad 2/(qp_{\mathrm{d}}(w^{1,2}))\big]^{\mathrm{T}}$. An allocation vector for a general REE procedure of class $\mathcal{D}$ is defined in the following.

Definition 9 (Allocation Vector): Let $\boldsymbol{w}$ represent a CQP fidelity vector on a chain $l_1:l_2$ and let $\boldsymbol{u}$ represent an REE procedure of class $\mathcal{D}$ on this chain. Define the allocation vector $\boldsymbol{v}_{\boldsymbol{u}}(\boldsymbol{w})$ in a recursive manner as follows.

- If $l_2-l_1=1$, then $\boldsymbol{u}=\mathbf{d}_c^{l_1,l_2}$ for some $c\in\mathbb{N}$. In this case,

$$\boldsymbol{v}_{\boldsymbol{u}}(\boldsymbol{w}):=\frac{1}{\beta\big(c,w^{l_1,l_2}\big)}\,. \tag{23}$$

- If $l_2-l_1>1$, then $\boldsymbol{u}$ can be written as in (8). In this case,

$$\boldsymbol{v}_{\boldsymbol{u}}(\boldsymbol{w}):=\frac{1}{q}\big[\boldsymbol{v}_{\boldsymbol{u}_{\mathrm{L}}}(\boldsymbol{w}_{\mathrm{L}})\quad\boldsymbol{v}_{\boldsymbol{u}_{\mathrm{R}}}(\boldsymbol{w}_{\mathrm{R}})\big]^{\mathrm{T}}\frac{1}{\beta\big(c,g_{\check{\boldsymbol{u}}}(\boldsymbol{w})\big)} \tag{24}$$

where $\boldsymbol{w}_{\mathrm{L}}$ and $\boldsymbol{w}_{\mathrm{R}}$ are defined in (10), and $\check{\boldsymbol{u}}$ is defined in (13).

□

D. Asymptotically Achievable Upper Bound on REE Rate

Consider a chain $0:L$ with CQP budget vector $\boldsymbol{b}$, CQP fidelity vector $\boldsymbol{w}$, and EQP fidelity threshold $\underline{w}$. Let M

represent the number of efficient REE procedures for $\boldsymbol{w}$ and $\underline{w}$. Moreover, let $\boldsymbol{u}^{(m)}$ represent the mth efficient REE procedure when the M efficient REE procedures are ordered according to an arbitrary criterion. The next theorem presents an upper bound on the optimal REE rate $r^*(\boldsymbol{b}, \boldsymbol{w})$ and shows that it can be achieved asymptotically.

Theorem 1: The optimal REE rate satisfies

$$r^*(\boldsymbol{b}, \boldsymbol{w}) \leqslant \hat{r} \tag{25}$$

where $-\hat{r}$ is the optimal objective value of the following linear program

$$\begin{aligned} \mathscr{P}: \ \underset{\boldsymbol{x}}{\text{minimize}} \quad & -L\left(\mathbf{1}^{\mathrm{T}}\boldsymbol{x}\right) && \text{(26a)} \\ \text{subject to} \quad & \boldsymbol{x} \succcurlyeq \mathbf{0} && \text{(26b)} \\ & \sum_{m=1}^{M} [\boldsymbol{x}]_m \, \boldsymbol{v}_{\boldsymbol{u}^{(m)}}(\boldsymbol{w}) \preccurlyeq \frac{\boldsymbol{b}}{|\boldsymbol{b}|}. && \text{(26c)} \end{aligned}$$

Furthermore, this optimal rate is asymptotically achievable as the budget of CQPs for each elementary link becomes sufficiently large. Specifically, there exists a policy π such that

$$\lim_{t\to\infty} r_\pi(t\boldsymbol{b}, \boldsymbol{w}) = \lim_{t\to\infty} r^*(t\boldsymbol{b}, \boldsymbol{w}) = \hat{r}\,. \tag{27}$$

□

Proof: The upper bound (25) is proved in Appendix B. Here, policies that satisfy (27) are presented. These policies are designed using the solution $\boldsymbol{x}^*$ to the optimization problem $\mathscr{P}$. Specifically, denote by $\mathcal{M}^*$ the set of indices of the non-zero entries in $\boldsymbol{x}^*$, i.e., $\mathcal{M}^* := \{m \in \{1, 2, \ldots, M\} : [\boldsymbol{x}^*]_m > 0\}$. Without loss of generality, assume that $\mathcal{M}^* = \{1, 2, \ldots, M^*\}$ for some positive integer $M^* \leqslant M$. The designed policy π for a given CQP budget vector $\boldsymbol{b}$ consists of M^* iterations. In the mth iteration with $m = 1, 2, \ldots, M^*$, CQPs are generated over elementary links of the chain according to CQP number vector $\left\lfloor t\,|\boldsymbol{b}|\,[\boldsymbol{x}^*]_m \boldsymbol{v}_{\boldsymbol{u}^{(m)}}(\boldsymbol{w})\right\rfloor$. In other words, for any $l = 1, 2, \ldots, L$, a total number of $\left\lfloor t\,|\boldsymbol{b}|\,[\boldsymbol{x}^*]_m \left[\boldsymbol{v}_{\boldsymbol{u}^{(m)}}(\boldsymbol{w})\right]_l\right\rfloor$ CQPs are generated over $(l-1, l)$ in the mth iteration. The nodes on the chain then perform the mth efficient REE procedure $\boldsymbol{u}^{(m)}$ by consuming the generated CQPs. Note that this policy satisfies the budget constraint since

$$\sum_{m=1}^{M^*} \left\lfloor t\,|\boldsymbol{b}|\,[\boldsymbol{x}^*]_m \boldsymbol{v}_{\boldsymbol{u}^{(m)}}(\boldsymbol{w})\right\rfloor \preccurlyeq \sum_{m=1}^{M^*} t\,|\boldsymbol{b}|\,[\boldsymbol{x}^*]_m \boldsymbol{v}_{\boldsymbol{u}^{(m)}}(\boldsymbol{w}) \preccurlyeq t\boldsymbol{b}$$

where the last inequality is obtained using (26c). In Appendix B, it is proved that policy π satisfies (27). ☒

Remark 4: Using results on linear optimization [92], the following conclusions can be drawn.

- The upper bound $\hat{r}$ is a function of the normalized CQP budget vector $\boldsymbol{b}/|\boldsymbol{b}|$ and of the CQP fidelity vector $\boldsymbol{w}$.
- The cardinality M^* of $\mathcal{M}^*$ introduced in the proof of the theorem satisfies $M^* \leqslant L$. In other words, the number of REE procedures employed in the designed policy is at most equal to the length of the chain irrespective of the number M of efficient REE procedures. This indicates that only a small portion of efficient REE procedures are selected if M is large.

□

Remark 5: While the upper bound presented in Theorem 1 is achievable in the asymptotic regime, its significance for the non-asymptotic regime is two-fold. First, it is still an upper bound on the REE rate. Second, the policy π presented in the proof of Theorem 1 can be employed as a near-optimal REE policy. The performance of this policy in the non-asymptotic regime is evaluated in the next section. □

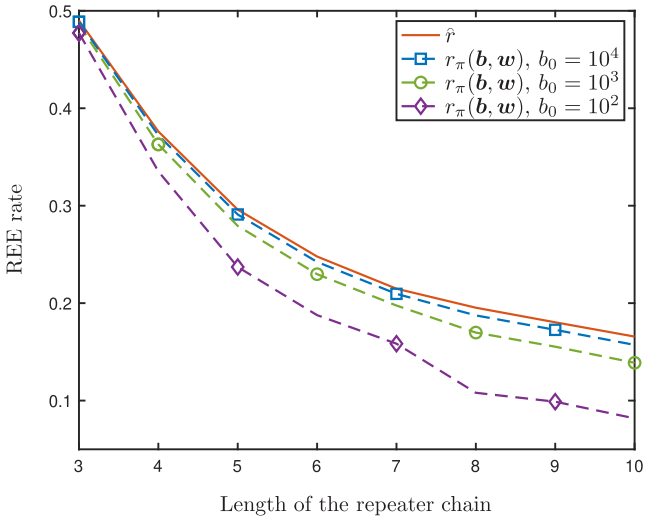

Fig. 3. REE rates with respect to the lengths of the chain for different values of CQP budget b_0. The solid orange curve represents the upper bounds on optimal REE rates shown in Theorem 1. The three dashed curves represent the REE rates $r_\pi(\boldsymbol{b}, \boldsymbol{w})$ achieved by policy π described in the proof of Theorem 1, for CQP budget vector $\boldsymbol{b} = b_0\mathbf{1}$ and CQP fidelity vector $\boldsymbol{w} = w_0\mathbf{1}$. Here, b_0 and w_0 represent the budget of CQPs and their fidelity for each elementary link of the chain.

IV. Numerical Results

The upper bounds on the optimal REE rates and the REE rates of the policy π presented in the proof of Theorem 1 are evaluated numerically in this section. In particular, the upper bounds are computed by solving the linear program (26c) via the dual-simplex algorithm [92], [93], [94], whereas the REE rates of π are computed via Monte-Carlo simulations. This section considers homogeneous chains such that the budget and fidelity of the CQPs for all elementary links of the chain are identical. In other words, the CQP budget vector $\boldsymbol{b}$ and CQP fidelity vector $\boldsymbol{w}$ can be written as $\boldsymbol{b} = b_0\mathbf{1}$ and $\boldsymbol{w} = w_0\mathbf{1}$, respectively, for $b_0 \in \mathbb{N}$ and $1/2 < w_0 \leqslant 1$. Specifically, the fidelity of CQPs is set to $w_0 = 0.95$, and the fidelity threshold of EQPs is set to $\underline{w} = 0.85$.

Figure 3 shows the upper bounds $\hat{r}$ of the optimal REE rates and the REE rates $r_\pi(\boldsymbol{b}, \boldsymbol{w})$ of the policy π designed in the proof of Theorem 1 with respect to the length L of the chain for $b_0 = 10^2, 10^3, 10^4$ and success probability of swapping $q = 0.7$. Both the upper bound and the REE rates decrease with respect to the length of the chain. In fact, more swapping operations are needed for establishing EQPs on longer chains. The effect on the number of EQPs is twofold. First, fewer qubit pairs are kept due to the failure of the swapping operations. Second, since swapping reduces fidelity, more distillation operations are required on longer chains to satisfy the fidelity requirement on the EQPs. Consequently, fewer qubit pairs are kept since two qubit pairs are consumed to create one distilled qubit pair and distillation can fail. In addition, as the budget b_0 of CQPs increases, the REE rates

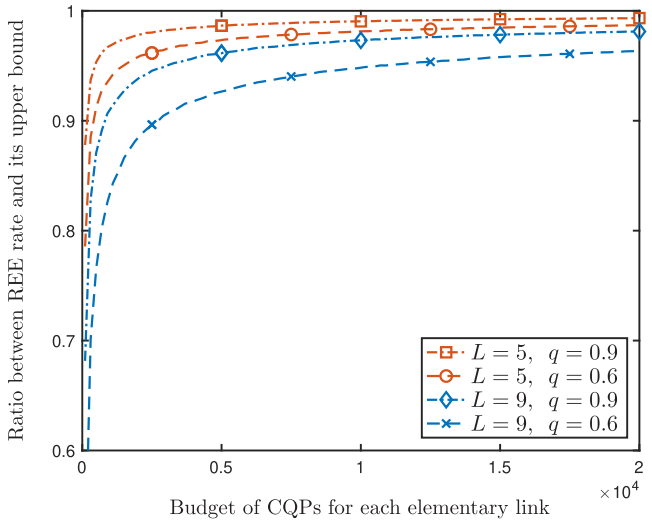

Fig. 4. Ratios between REE rates $r_\pi(\boldsymbol{b}, \boldsymbol{w})$ and the upper bounds $\hat{r}$ on optimal REE rates with respect to the budget of CQPs for each elementary link. Different values of chain length L and success probability of swapping q are considered.

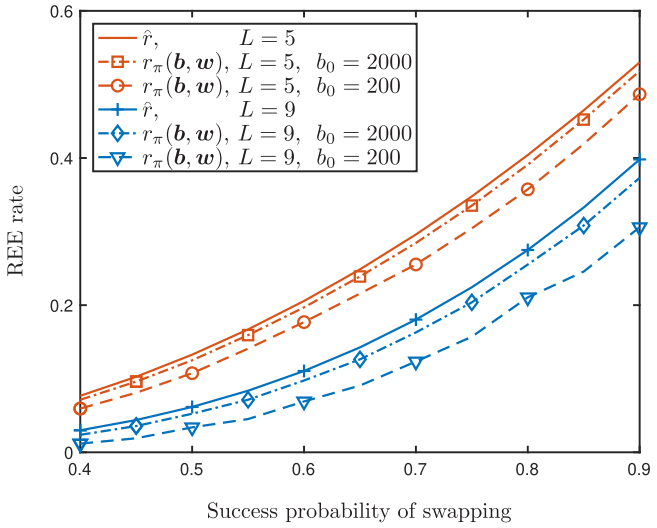

Fig. 5. REE rates with respect to the success probabilities of swapping for different values of chain length L and different values of budget b_0 of CQPs for each elementary link. The solid curves represent the upper bounds on optimal REE rates. The dashed and dash-dotted curves represent the REE rates $r_\pi(\boldsymbol{b}, \boldsymbol{w})$ achieved by policy π described in the proof of Theorem 1.

of the designed policy approach the upper bounds for different lengths of the chains.

Figure 4 shows the ratio $r_\pi(\boldsymbol{b}, \boldsymbol{w})/\hat{r}$ with respect to b_0 for $L = 5, 9$ and $q = 0.6, 0.9$. The ratio increases and approaches 1 as b_0 becomes larger. This corroborates the assertion in Theorem 1 that policy π achieves the upper bounds on optimal REE rates asymptotically. Also, the REE rates of π approach the upper bounds more slowly for longer chains and for lower success probability of swapping. In particular, in order for $r_\pi(\boldsymbol{b}, \boldsymbol{w})/\hat{r}$ to achieve the value 0.95, the minimum budgets b_0 are 5×10^2 and 15×10^2, respectively, for $q = 0.9$ and $q = 0.6$ when the length of the chain is $L = 5$, whereas the minimum budgets are 30×10^2 and 107×10^2, respectively, for $q = 0.9$ and $q = 0.6$ when the length of the chain is $L = 9$. This can be explained as follows. According to law of large numbers (see Appendix B), the REE rates of π approach the upper bounds in the asymptotic regime, i.e., when the budget of CQPs for each elementary link becomes sufficiently large. As the chain becomes longer and as the success probability of swapping becomes lower, fewer EQPs can be established since more distillation operations are required and more swapping failures happen. Consequently, higher budgets on CQPs are needed in order to achieve the upper bounds on the REE rates.

Figure 5 shows $\hat{r}$ and $r_\pi(\boldsymbol{b}, \boldsymbol{w})$ with respect to the success probability of swapping q for chain length $L = 5, 9$ and budget of CQPs $b_0 = 200, 2000$. First, both the upper bounds on optimal REE rates and the REE rates of π increase significantly with respect to q. In particular, when q changes from 0.5 to 0.9, the upper bound increases from 0.13 to 0.53 on a chain with length $L = 5$ and increases from 0.06 to 0.40 on a chain with length $L = 9$. Second, the gaps between REE rates of π and the upper bounds drop significantly when $b_0 = 2000$ compared to $b_0 = 200$ for both $L = 5$ and $L = 9$ and all values of q.

V. Conclusion

This paper developed a theoretical framework for establishing high-fidelity entanglement in quantum repeater chains. In particular, the paper derived an upper bound of the optimal rate at which EQPs between a source node and a destination node can be created with minimum fidelity requirements. Methods used for deriving this bound include employing the notions of enode graphs and REE procedures, and converting the REE problem into a linear program via certainty equivalence. Based on the solution to the linear program, an REE policy was designed and its rate was shown to achieve the derived upper bound asymptotically. In particular, this policy contains multiple iterations, where a proportion of the CQP budget is consumed in each iteration to perform an REE procedure. This paper demonstrates the benefits of employing optimized quantum operation sequences on REE performance and provides guidelines for the development of communication protocols in the quantum internet.

Appendix A
Proof of Proposition 2

First, a lemma to be used in the proof is presented.

Lemma 1: Consider a chain $0:2$ as well as two REE procedures on this chain $\boldsymbol{u} := \left(\mathrm{s}^{0,1,2}, \mathbf{d}_c^{0,2}\right)$ and $\boldsymbol{u}' := \left(\mathbf{d}_c^{0,1}, \mathbf{d}_c^{1,2}, \mathrm{s}^{0,1,2}\right)$, where $c \in \mathbb{N}$. Then for any CQP number vector $\boldsymbol{n}$ and CQP fidelity vector $\boldsymbol{w}$ on this chain, it holds that

$$g_{\boldsymbol{u}'}(\boldsymbol{w}) \geqslant g_{\boldsymbol{u}}(\boldsymbol{w}) \tag{28a}$$

$$\zeta_{\boldsymbol{u}'}(\boldsymbol{n}, \boldsymbol{w}) \geqslant \zeta_{\boldsymbol{u}}(\boldsymbol{n}, \boldsymbol{w})\,. \tag{28b}$$

□

Proof: Note that $\boldsymbol{u} = \boldsymbol{u}'$ if $c = 0$ and thus only the case that $c > 0$ needs to be considered. We first show (28a) for the case $c = 1$. Calculation based on (3) and (4) gives

$$\begin{aligned} g_{\boldsymbol{u}'}(\boldsymbol{w}) &= g_{\mathrm{s}}\big(g_{\mathrm{d}}(w^{0,1}),\, g_{\mathrm{d}}(w^{1,2})\big) \\ &= \frac{1}{2} + \frac{2(2w^{0,1}-1)(2w^{1,2}-1)}{[(2w^{0,1}-1)^2+1][(2w^{1,2}-1)^2+1]} \end{aligned} \tag{29a}$$

$$\begin{aligned} g_{\boldsymbol{u}}(\boldsymbol{w}) &= g_{\mathrm{d}}\big(g_{\mathrm{s}}(w^{0,1}, w^{1,2})\big) \\ &= \frac{1}{2} + \frac{2(2w^{0,1}-1)(2w^{1,2}-1)}{2(2w^{0,1}-1)^2(2w^{1,2}-1)^2+2}\,. \end{aligned} \tag{29b}$$

The difference between the denominator in the second term of (29b) and that of (29a) can be shown to be

$$\left[(2w^{0,1}-1)^2-1\right]\left[(2w^{1,2}-1)^2-1\right]\geqslant 0$$

where the inequality is obtained using $1/2<w^{0,1},w^{1,2}\leqslant 1$. This shows that (28a) holds for $c=1$. Consider the case that $c>1$. Note that

$$g_{\boldsymbol{u}'}(\boldsymbol{w})=g_{\mathrm{s}}\big(g_{\mathrm{d}}^{\circ c}(w^{0,1}),\, g_{\mathrm{d}}^{\circ c}(w^{1,2})\big).$$

Applying (28a) for the case $c=1$ with CQP fidelity vector $\left[g_{\mathrm{d}}^{\circ(c-1)}(w^{0,1})\quad g_{\mathrm{d}}^{\circ(c-1)}(w^{1,2})\right]^{\mathrm{T}}$ gives

$$g_{\boldsymbol{u}'}(\boldsymbol{w})\geqslant g_{\mathrm{d}}\big(g_{\mathrm{s}}\big(g_{\mathrm{d}}^{\circ(c-1)}(w^{0,1}),\, g_{\mathrm{d}}^{\circ(c-1)}(w^{1,2})\big)\big)\,.$$

Repeating this procedure for $c-1$ more times gives

$$g_{\boldsymbol{u}'}(\boldsymbol{w})\geqslant g_{\mathrm{d}}^{\circ c}\big(g_{\mathrm{s}}\big(w^{0,1},\, w^{1,2}\big)\big)=g_{\boldsymbol{u}}(\boldsymbol{w})$$

and thus (28a) is proved for general $c\in\mathbb{N}$.

Next,(28b) is proved for $c>0$. Applying Definition 6,

$$\zeta_{\boldsymbol{u}'}(\boldsymbol{n},\boldsymbol{w})=q\min\big\{\beta(c,w^{0,1})n^{0,1},\,\beta(c,w^{1,2})n^{1,2}\big\} \quad (30a)$$

$$\zeta_{\boldsymbol{u}}(\boldsymbol{n},\boldsymbol{w})=q\,\beta\big(c,g_{\mathrm{s}}(w^{0,1},w^{1,2})\big)\,\min\{n^{0,1},n^{0,2}\}\,. \quad (30b)$$

Since swapping does not increase fidelity, it holds that $g_{\mathrm{s}}(w^{0,1},w^{1,2})\leqslant\min\{w^{0,1},w^{1,2}\}$. Combining (18) with (2) and (3), we can verify that $\beta(\cdot,\cdot)$ is monotonically non-decreasing with respect to the second argument. Therefore, $\beta\big(c,g_{\mathrm{s}}(w^{0,1},w^{1,2})\big)\leqslant\min\big\{\beta(c,w^{0,1}),\,\beta(c,w^{1,2})\big\}$. Combining this with (30) gives (28b). The desired results are thus proved. ⊠

Remark 6: Note that distillation is performed after swapping in $\boldsymbol{u}$ and before swapping in $\boldsymbol{u}'$. Lemma 1 shows that in a chain of length 2, compared to the REE procedure where distillation is performed after swapping, performing distillation before swapping establishes qubit pairs between nodes 0 and 2 with higher fidelity and the number of the established qubit pairs is larger under CE. This corroborates the results in [95]. □

Next, Proposition 2 is proved.

Proof: Let $\boldsymbol{w}$ be an arbitrary CQP fidelity vector on the chain and let $\boldsymbol{u}$ represent a feasible REE procedure for $\boldsymbol{w}$ and fidelity threshold $\underline{w}$. We show via strong mathematical induction [96] that there exists an REE procedure $\boldsymbol{u}'$ of class $\mathcal{D}$ such that

$$g_{\boldsymbol{u}'}(\boldsymbol{w})\geqslant g_{\boldsymbol{u}}(\boldsymbol{w}) \quad (31a)$$

$$\zeta_{\boldsymbol{u}'}(\boldsymbol{n},\boldsymbol{w})\geqslant\zeta_{\boldsymbol{u}}(\boldsymbol{n},\boldsymbol{w})\,,\qquad\forall\boldsymbol{n}\succcurlyeq\boldsymbol{0}\,. \quad (31b)$$

In particular, (31a) indicates that $\boldsymbol{u}'$ is also feasible. Therefore, if $\boldsymbol{u}$ is not of class $\mathcal{D}$, then $\boldsymbol{u}'$ is different from $\boldsymbol{u}$ and thus $\boldsymbol{u}$ is not efficient.

For the base case of the induction, consider a chain $l_1:l_2$ with length $l_2-l_1=1$. For this case, all the REE procedures, including efficient REE procedures, consist of only distillation operations over the elementary link (l_1,l_2) and therefore must be of class $\mathcal{D}$. Consequently, the base case of the induction is proved.

For the induction step, suppose that (31) has been proved for chains with lengths $1,2,\ldots,L-1$, and we prove it for a chain $l_1:l_2$ with length $l_2-l_1=L$. Write the REE procedure $\boldsymbol{u}$ as in (8). Define REE procedure $\boldsymbol{u}^{(1)}:=\big(\boldsymbol{u}_{\mathrm{L}},\mathbf{d}_c^{l_1,l},\,\boldsymbol{u}_{\mathrm{R}},\mathbf{d}_c^{l,l_2},\,\mathrm{s}^{l_1,l,l_2}\big)$. Define $\boldsymbol{w}_{\mathrm{L}}$, $\boldsymbol{w}_{\mathrm{R}}$, $\boldsymbol{n}_{\mathrm{R}}$, and $\boldsymbol{n}_{\mathrm{L}}$ as in (10) and (12). Applying Lemma 1 by replacing $\boldsymbol{w}$ in (28a) with $\left[g_{\boldsymbol{u}_{\mathrm{L}}}(\boldsymbol{w}_{\mathrm{L}})\quad g_{\boldsymbol{u}_{\mathrm{R}}}(\boldsymbol{w}_{\mathrm{R}})\right]^{\mathrm{T}}$ gives $g_{\boldsymbol{u}^{(1)}}(\boldsymbol{w})\geqslant g_{\boldsymbol{u}}(\boldsymbol{w})$. Define $\boldsymbol{u}_{\mathrm{L}}^{(1)}:=(\boldsymbol{u}_{\mathrm{L}},\mathbf{d}_c^{l_1,l})$, which is an REE procedure on $l_1:l$ with length $l-l_1<L$. By induction hypothesis, there exists an REE procedure $\boldsymbol{u}'_{\mathrm{L}}$ of class $\mathcal{D}$ on chain $l_1:l$ such that

$$g_{\boldsymbol{u}'_{\mathrm{L}}}(\boldsymbol{w}_{\mathrm{L}})\geqslant g_{\boldsymbol{u}_{\mathrm{L}}^{(1)}}(\boldsymbol{w}_{\mathrm{L}}) \quad (32a)$$

$$\zeta_{\boldsymbol{u}'_{\mathrm{L}}}(\boldsymbol{n}_{\mathrm{L}},\boldsymbol{w}_{\mathrm{L}})\geqslant\zeta_{\boldsymbol{u}_{\mathrm{L}}^{(1)}}(\boldsymbol{n}_{\mathrm{L}},\boldsymbol{w}_{\mathrm{L}})\,. \quad (32b)$$

Similarly, define $\boldsymbol{u}_{\mathrm{R}}^{(1)}=\big(\boldsymbol{u}_{\mathrm{R}},\mathbf{d}_c^{l,l_2}\big)$. There exists an REE procedure $\boldsymbol{u}'_{\mathrm{R}}$ of class $\mathcal{D}$ on $l:l_2$ such that

$$g_{\boldsymbol{u}'_{\mathrm{R}}}(\boldsymbol{w}_{\mathrm{R}})\geqslant g_{\boldsymbol{u}_{\mathrm{R}}^{(1)}}(\boldsymbol{w}_{\mathrm{R}}) \quad (33a)$$

$$\zeta_{\boldsymbol{u}'_{\mathrm{R}}}(\boldsymbol{n}_{\mathrm{R}},\boldsymbol{w}_{\mathrm{R}})\geqslant\zeta_{\boldsymbol{u}_{\mathrm{R}}^{(1)}}(\boldsymbol{n}_{\mathrm{R}},\boldsymbol{w}_{\mathrm{R}})\,. \quad (33b)$$

Define $\boldsymbol{u}':=\big(\boldsymbol{u}'_{\mathrm{L}},\,\boldsymbol{u}'_{\mathrm{R}},\,\mathrm{s}^{l_1,l,l_2}\big)$. By definition, $\boldsymbol{u}'$ is an REE procedure of class $\mathcal{D}$ on $l_1:l_2$. Moreover, combining (32a) and (33a) gives

$$\begin{aligned}g_{\boldsymbol{u}'}(\boldsymbol{w})&=g_{\mathrm{s}}\big(g_{\boldsymbol{u}'_{\mathrm{L}}}(\boldsymbol{w}_{\mathrm{L}}),\,g_{\boldsymbol{u}'_{\mathrm{R}}}(\boldsymbol{w}_{\mathrm{R}})\big)\\&\geqslant g_{\mathrm{s}}\big(g_{\boldsymbol{u}_{\mathrm{L}}^{(1)}}(\boldsymbol{w}_{\mathrm{L}}),\,g_{\boldsymbol{u}_{\mathrm{R}}^{(1)}}(\boldsymbol{w}_{\mathrm{R}})\big)=g_{\boldsymbol{u}^{(1)}}(\boldsymbol{w})\,.\end{aligned}$$

Combining this with $g_{\boldsymbol{u}^{(1)}}(\boldsymbol{w})\geqslant g_{\boldsymbol{u}}(\boldsymbol{w})$ gives (31a). Similarly, (31b) can also be shown. Consequently, the induction step is complete, and thus the proposition is proved. ⊠

Appendix B
Proof of Theorem 1

To prove the theorem, the notion of allocation scaling factor is introduced.

Definition 10 (Allocation Scaling Factor): Let $\boldsymbol{n}$ and $\boldsymbol{w}$ represent a CQP number vector and a CQP fidelity vector, respectively, on a chain. Moreover, let $\boldsymbol{u}$ represent an REE procedure of class $\mathcal{D}$ on this chain. The allocation scaling factor $\alpha_{\boldsymbol{u}}(\boldsymbol{n},\boldsymbol{w})$ is defined as the maximum real number that can be multiplied by $\boldsymbol{v}_{\boldsymbol{u}}(\boldsymbol{w})$ so that the product is smaller than or equal to $\boldsymbol{n}$ entry-wise, i.e.,

$$\alpha_{\boldsymbol{u}}(\boldsymbol{n},\boldsymbol{w}):=\max\big\{x\in\mathbb{R}:\,x\,\boldsymbol{v}_{\boldsymbol{u}}(\boldsymbol{w})\preccurlyeq\boldsymbol{n}\big\}\,. \quad (34)$$

□

The next lemma shows the relationship between the number of established qubit pairs under CE and the allocation scaling factor.

Lemma 2: For an arbitrary CQP number vector $\boldsymbol{n}$, CQP fidelity vector $\boldsymbol{w}$, and REE procedure $\boldsymbol{u}$ of class $\mathcal{D}$ on a chain, the following equality holds

$$\zeta_{\boldsymbol{u}}(\boldsymbol{n},\boldsymbol{w})=\alpha_{\boldsymbol{u}}(\boldsymbol{n},\boldsymbol{w})\,. \quad (35)$$

□

Proof: The lemma is proved via induction. For the base case, consider a chain $l_1:l_2$ with length $l_2-l_1=1$. For this case, $\boldsymbol{u}=\mathbf{d}_c^{l_1,l_2}$ for some $c\in\mathbb{N}$. Combining (20) and (23) gives $\alpha_{\boldsymbol{u}}(\boldsymbol{n},\boldsymbol{w})=\beta\big(c,w^{l_1,l_2}\big)n^{l_1,l_2}=\zeta_{\boldsymbol{u}}(\boldsymbol{n},\boldsymbol{w})$. Consequently, the base case of the induction is proved. For the induction step, suppose that (35) holds for chains with lengths $1,2,\ldots,L-1$, and we prove next that it also holds for $l_2-l_1=L$. Write REE procedure $\boldsymbol{u}$ as in (8). Then $\zeta_{\boldsymbol{u}}(\boldsymbol{n},\boldsymbol{w})$ can be written as

in (21). Applying induction hypothesis on $\zeta_{\boldsymbol{u}_{\mathrm{L}}}(\boldsymbol{n}_{\mathrm{L}}, \boldsymbol{w}_{\mathrm{L}})$ and $\zeta_{\boldsymbol{u}_{\mathrm{R}}}(\boldsymbol{n}_{\mathrm{R}}, \boldsymbol{w}_{\mathrm{R}})$ gives

$$\zeta_{\boldsymbol{u}}(\boldsymbol{n}, \boldsymbol{w}) = q \min\big\{\alpha_{\boldsymbol{u}_{\mathrm{L}}}(\boldsymbol{n}_{\mathrm{L}}, \boldsymbol{w}_{\mathrm{L}}), \alpha_{\boldsymbol{u}_{\mathrm{R}}}(\boldsymbol{n}_{\mathrm{R}}, \boldsymbol{w}_{\mathrm{R}})\big\} \times \beta\big(c, g_{\breve{\boldsymbol{u}}}(\boldsymbol{w})\big) \tag{36}$$

where $\breve{\boldsymbol{u}}$ is defined in (13). On the other hand, using (34) gives $\alpha_{\boldsymbol{u}}(\boldsymbol{n}, \boldsymbol{w}) = \min\{x_{\mathrm{L}}, x_{\mathrm{R}}\}$, where

$$x_{\mathrm{L}} := \max\big\{x \in \mathbb{R} : x\big[\boldsymbol{v}_{\boldsymbol{u}}(\boldsymbol{w})\big]_{1:l-l_1} \preccurlyeq \boldsymbol{n}_{\mathrm{L}}\big\}$$
$$x_{\mathrm{R}} := \max\big\{x \in \mathbb{R} : x\big[\boldsymbol{v}_{\boldsymbol{u}}(\boldsymbol{w})\big]_{l-l_1+1:l_2-l_1} \preccurlyeq \boldsymbol{n}_{\mathrm{R}}\big\}.$$

Equation (24) gives the equality $\big[\boldsymbol{v}_{\boldsymbol{u}}(\boldsymbol{w})\big]_{1:l-l_1} = \boldsymbol{v}_{\boldsymbol{u}_{\mathrm{L}}}(\boldsymbol{w}_{\mathrm{L}})/\big(q\beta\big(c, g_{\breve{\boldsymbol{u}}}(\boldsymbol{w})\big)\big)$. Combining this equality with (34) gives $x_{\mathrm{L}} = q\beta\big(c, g_{\breve{\boldsymbol{u}}}(\boldsymbol{w})\big)\alpha_{\boldsymbol{u}_{\mathrm{L}}}(\boldsymbol{n}_{\mathrm{L}}, \boldsymbol{w}_{\mathrm{L}})$. Similarly, $x_{\mathrm{R}} = q\beta\big(c, g_{\breve{\boldsymbol{u}}}(\boldsymbol{w})\big)\alpha_{\boldsymbol{u}_{\mathrm{R}}}(\boldsymbol{n}_{\mathrm{R}}, \boldsymbol{w}_{\mathrm{R}})$. Combining these two equalities with (36) gives $\zeta_{\boldsymbol{u}}(\boldsymbol{n}, \boldsymbol{w}) = \min\{x_{\mathrm{L}}, x_{\mathrm{R}}\}$. Combining this with $\alpha_{\boldsymbol{u}}(\boldsymbol{n}, \boldsymbol{w}) = \min\{x_{\mathrm{L}}, x_{\mathrm{R}}\}$ gives $\alpha_{\boldsymbol{u}}(\boldsymbol{n}, \boldsymbol{w}) = \zeta_{\boldsymbol{u}}(\boldsymbol{n}, \boldsymbol{w})$, and thus the induction step is complete. ⊠

Remark 7: Lemma 2 shows an efficient method for allocating CQPs under CE. Specifically, combining (34) and (35) gives

$$\zeta_{\boldsymbol{u}}(x\,\boldsymbol{v}_{\boldsymbol{u}}(\boldsymbol{w}), \boldsymbol{w}) = x \tag{37}$$
$$\zeta_{\boldsymbol{u}}(\boldsymbol{n}, \boldsymbol{w}) < x \quad \forall \boldsymbol{n} \preccurlyeq x\,\boldsymbol{v}_{\boldsymbol{u}}(\boldsymbol{w}) \ \text{ and } \ \boldsymbol{n} \neq x\,\boldsymbol{v}_{\boldsymbol{u}}(\boldsymbol{w}). \tag{38}$$

Equality (37) shows that to establish x qubit pairs between the source node and the destination node, the required number of CQPs of the ith elementary link under CE can be represented by the ith entry of the CQP number vector $x\,\boldsymbol{v}_{\boldsymbol{u}}(\boldsymbol{w})$. Inequality (38) shows that if any entry of $x\,\boldsymbol{v}_{\boldsymbol{u}}(\boldsymbol{w})$ is reduced, then the number of established qubit pairs would be smaller than x. This shows that all the CQPs generated according to $x\,\boldsymbol{v}_{\boldsymbol{u}}(\boldsymbol{w})$ are necessary under CE for establishing x qubit pairs. □

Next, Theorem 1 is proved.

Proof: First, (25) is proved. Combining (16) with (6) and using $l_2 - l_1 = L$ show that $r^*(\boldsymbol{b}, \boldsymbol{w})$ is the optimal objective value of the following optimization problem

$$\begin{aligned} \underset{\{K, \{\boldsymbol{n}_k, \boldsymbol{u}_k\}_{k=1}^K\}}{\text{maximize}} \quad & \frac{L}{|\boldsymbol{b}|}\sum_{k=1}^{K} \mathbb{E}\big\{\check{\mathrm{z}}_{\boldsymbol{u}_k}(\boldsymbol{n}_k, \boldsymbol{w})\big\} \\ \text{subject to} \quad & \boldsymbol{n}_k \in \mathbb{N}^{l_2-l_1}, \quad \forall k = 1, 2, \ldots, K \\ & \sum_{k=1}^{K} \boldsymbol{n}_k \preccurlyeq \boldsymbol{b}. \end{aligned} \tag{39}$$

This problem optimizes over the total number of iterations K as well as the generation vector $\boldsymbol{n}_k$ and REE procedure $\boldsymbol{u}_k$ for each iteration. Applying (22) in Proposition 1, and applying convex relaxation by substituting $\boldsymbol{n}_k \in \mathbb{N}^{l_2-l_1}$ in (39) with $\boldsymbol{n}_k \succcurlyeq \boldsymbol{0}$, we obtain an upper bound on $r^*(\boldsymbol{b}, \boldsymbol{w})$. Specifically,

$$r^*(\boldsymbol{b}, \boldsymbol{w}) \leqslant r_1 \tag{40}$$

where r_1 is the optimal objective value of the following optimization problem $\mathscr{P}_1$

$$\begin{aligned} \mathscr{P}_1: \ \underset{\{K, \{\boldsymbol{n}_k, \boldsymbol{u}_k\}_{k=1}^K\}}{\text{maximize}} \quad & \frac{L}{|\boldsymbol{b}|}\sum_{k=1}^{K} \zeta_{\boldsymbol{u}_k}(\boldsymbol{n}_k, \boldsymbol{w}) \\ \text{subject to} \quad & \boldsymbol{n}_k \succcurlyeq \boldsymbol{0}, \quad \forall k = 1, 2, \ldots, K \\ & \sum_{k=1}^{K} \boldsymbol{n}_k \preccurlyeq \boldsymbol{b}. \end{aligned}$$

In $\mathscr{P}_1$, we can require that each REE procedure $\boldsymbol{u}_k$ be efficient under CE (see Definition 7). In particular, if any $\boldsymbol{u}_k$ is not efficient, then there exists a feasible REE procedure $\boldsymbol{u}'_k \neq \boldsymbol{u}_k$ such that $\zeta_{\boldsymbol{u}'_k}(\boldsymbol{n}_k, \boldsymbol{w}) \geqslant \zeta_{\boldsymbol{u}_k}(\boldsymbol{n}_k, \boldsymbol{w})$. Therefore, if $\boldsymbol{u}_k$ is replaced by $\boldsymbol{u}'_k$, then the objective value of $\mathscr{P}_1$ is guaranteed not to decrease while all the constraints are satisfied. Consequently, it can be required that $\boldsymbol{u}_k$ is efficient under CE for all $k = 1, 2, \ldots, K$. Combine the iterations where the same efficient REE procedure is used by defining $\breve{\boldsymbol{n}}^{(m)} := \sum_{k=1}^{K} \mathbb{1}_{\{\boldsymbol{u}^{(m)}\}}(\boldsymbol{u}_k)\,\boldsymbol{n}_k$. Here, $\mathbb{1}_{\mathcal{X}}(x)$ represents the indicator function such that $\mathbb{1}_{\mathcal{X}}(x) = 1$ if $x \in \mathcal{X}$ and $\mathbb{1}_{\mathcal{X}}(x) = 0$ otherwise. Then optimization problem $\mathscr{P}_1$ can be replaced by an equivalent optimization problem $\mathscr{P}_2$ given by

$$\mathscr{P}_2: \ \underset{\{\breve{\boldsymbol{n}}^{(m)}\}_{m=1}^M}{\text{maximize}} \quad \frac{L}{|\boldsymbol{b}|}\sum_{m=1}^{M} \zeta_{\boldsymbol{u}^{(m)}}\big(\breve{\boldsymbol{n}}^{(m)}, \boldsymbol{w}\big) \tag{41a}$$
$$\text{subject to} \quad \breve{\boldsymbol{n}}^{(m)} \succcurlyeq \boldsymbol{0}, \quad \forall m = 1, 2, \ldots, M \tag{41b}$$
$$\sum_{m=1}^{M} \breve{\boldsymbol{n}}^{(m)} \preccurlyeq \boldsymbol{b}. \tag{41c}$$

Moreover, the optimal objective value r_2 of $\mathscr{P}_2$ can be shown to equal $\hat{r}$, i.e., the opposite of the optimal objective value for $\mathscr{P}$ given by (26c). To see this, let $\boldsymbol{x}^*$ represent the solution to $\mathscr{P}$. The collection of vectors

$$\big\{|\boldsymbol{b}|[\boldsymbol{x}^*]_1 \boldsymbol{v}_{\boldsymbol{u}^{(1)}}(\boldsymbol{w}),\ |\boldsymbol{b}|[\boldsymbol{x}^*]_2 \boldsymbol{v}_{\boldsymbol{u}^{(2)}}(\boldsymbol{w}), \ldots,\ |\boldsymbol{b}|[\boldsymbol{x}^*]_M \boldsymbol{v}_{\boldsymbol{u}^{(M)}}(\boldsymbol{w})\big\}$$

can be verified to be a feasible point for problem $\mathscr{P}_2$. Moreover, the objective function of $\mathscr{P}_2$ at this point equals $L(\boldsymbol{1}^{\mathrm{T}}\boldsymbol{x}^*)$. To see this, note that (37) gives

$$\zeta_{\boldsymbol{u}^{(m)}}\big([\boldsymbol{x}^*]_m\,\boldsymbol{v}_{\boldsymbol{u}^{(m)}}(\boldsymbol{w}),\ \boldsymbol{w}\big) = [\boldsymbol{x}^*]_m.$$

Since r_2 is the optimal objective value of $\mathscr{P}_2$,

$$r_2 \geqslant L(\boldsymbol{1}^{\mathrm{T}}\boldsymbol{x}^*) = \hat{r} \tag{42}$$

where the equality is obtained using (26a). On the other hand, let $\big\{\breve{\boldsymbol{n}}_*^{(1)}, \breve{\boldsymbol{n}}_*^{(2)}, \ldots, \breve{\boldsymbol{n}}_*^{(M)}\big\}$ represent a solution to $\mathscr{P}_2$. Define a vector $\boldsymbol{\alpha}$ as

$$\boldsymbol{\alpha} := \frac{1}{|\boldsymbol{b}|}\Big[\alpha_{\boldsymbol{u}^{(1)}}\big(\breve{\boldsymbol{n}}_*^{(1)}, \boldsymbol{w}\big)\ \alpha_{\boldsymbol{u}^{(2)}}\big(\breve{\boldsymbol{n}}_*^{(2)}, \boldsymbol{w}\big)\ \cdots\ \alpha_{\boldsymbol{u}^{(M)}}\big(\breve{\boldsymbol{n}}_*^{(M)}, \boldsymbol{w}\big)\Big]^{\mathrm{T}}$$

where $\alpha_{\boldsymbol{u}}(\boldsymbol{n}, \boldsymbol{w})$ represents the allocation scaling factor defined in Definition 10. By this definition, $\boldsymbol{\alpha} \succcurlyeq \mathbf{0}$. The same definition also shows that $\alpha_{\boldsymbol{u}^{(M)}}\left(\breve{\boldsymbol{n}}_*^{(M)}, \boldsymbol{w}\right) \boldsymbol{v}_{\boldsymbol{u}^{(m)}}(\boldsymbol{w}) \preccurlyeq \breve{\boldsymbol{n}}_*^{(m)}$ for $m = 1, 2, \ldots, M$. Combining these inequalities with constraint (41c) gives

$$\sum_{m=1}^{M} \frac{1}{|\boldsymbol{b}|} \alpha_{\boldsymbol{u}^{(M)}}\left(\breve{\boldsymbol{n}}_*^{(M)}, \boldsymbol{w}\right) \boldsymbol{v}_{\boldsymbol{u}^{(m)}}(\boldsymbol{w}) \preccurlyeq \sum_{m=1}^{M} \frac{1}{|\boldsymbol{b}|} \breve{\boldsymbol{n}}_*^{(m)} \preccurlyeq \frac{\boldsymbol{b}}{|\boldsymbol{b}|} .$$

This shows that $\boldsymbol{\alpha}$ is a feasible point for $\mathscr{P}$, and thus $-L(\mathbf{1}^{\mathrm{T}}\boldsymbol{\alpha}) \geqslant -L(\mathbf{1}^{\mathrm{T}}\boldsymbol{x}^*)$. Furthermore, applying Proposition 2 gives $\zeta_{\boldsymbol{u}^{(m)}}\left(\breve{\boldsymbol{n}}_*^{(m)}, \boldsymbol{w}\right) = \alpha_{\boldsymbol{u}^{(m)}}\left(\breve{\boldsymbol{n}}_*^{(m)}, \boldsymbol{w}\right)$, and thus the optimal objective value r_2 of $\mathscr{P}_2$ equals $L(\mathbf{1}^{\mathrm{T}}\boldsymbol{\alpha})$. Consequently, $r_2 = L(\mathbf{1}^{\mathrm{T}}\boldsymbol{\alpha}) \leqslant L(\mathbf{1}^{\mathrm{T}}\boldsymbol{x}^*) = \hat{r}$. Combining this with (42) gives $r_2 = \hat{r}$. Recalling that $\mathscr{P}_1$ is equivalent to $\mathscr{P}_2$, we obtain $r_1 = \hat{r}$. Substituting this into (40) gives the desired result (25).

Finally, (27) is proved. Using the strong law of large numbers [91], [97], we can show that as t approaches infinity,

$$\frac{1}{t|\boldsymbol{b}|} \check{\mathtt{z}}_{\boldsymbol{u}^{(m)}}\left(\left\lfloor t\,|\boldsymbol{b}|\,[\boldsymbol{x}^*]_m\, \boldsymbol{v}_{\boldsymbol{u}^{(m)}}(\boldsymbol{w})\right\rfloor, \boldsymbol{w}\right) \xrightarrow{\text{a.s.}} \zeta_{\boldsymbol{u}}([\boldsymbol{x}^*]_m\, \boldsymbol{v}_{\boldsymbol{u}^{(m)}}(\boldsymbol{w}), \boldsymbol{w}) = [\boldsymbol{x}^*]_m , \quad m = 1, 2, \ldots, M^*$$

where $\xrightarrow{\text{a.s.}}$ represents almost sure convergence, and the equality is obtained using (37). Applying the bounded convergence theorem, we obtain

$$\lim_{t\to\infty} \frac{1}{t|\boldsymbol{b}|} \mathbb{E}\left\{\check{\mathtt{z}}_{\boldsymbol{u}^{(m)}}\left(\left\lfloor t\,|\boldsymbol{b}|\,[\boldsymbol{x}^*]_m\, \boldsymbol{v}_{\boldsymbol{u}^{(m)}}(\boldsymbol{w})\right\rfloor, \boldsymbol{w}\right)\right\} = [\boldsymbol{x}^*]_m .$$

Combining this with the following equality

$$r_\pi(t\boldsymbol{b}, \boldsymbol{w}) = \frac{L}{t|\boldsymbol{b}|} \sum_{m=1}^{M^*} \mathbb{E}\left\{\check{\mathtt{z}}_{\boldsymbol{u}^{(m)}}\left(\left\lfloor t\,|\boldsymbol{b}|\,[\boldsymbol{x}^*]_m\, \boldsymbol{v}_{\boldsymbol{u}^{(m)}}(\boldsymbol{w})\right\rfloor, \boldsymbol{w}\right)\right\}$$

and noting that $\hat{r} = L\left(\mathbf{1}^{\mathrm{T}}\boldsymbol{x}^*\right)$ gives the desired result (27). ☒

ACKNOWLEDGMENT

The authors wish to thank M. Clouâtré, B. Kartal, and U. Keskin for their helpful suggestions and careful reading of the manuscript.

REFERENCES

[1] J. Preskill, "Quantum computing in the NISQ era and beyond," *Quantum*, vol. 2, p. 79, Aug. 2018.

[2] J. P. Dowling and G. J. Milburn, "Quantum technology: The second quantum revolution," *Philos. Trans. Royal Soc. A, Math., Phys. Eng. Sci.*, vol. 361, no. 1809, pp. 1655–1674, Jun. 2003.

[3] J. Illiano, M. Caleffi, A. Manzalini, and A. S. Cacciapuoti, "Quantum internet protocol stack: A comprehensive survey," *Comput. Netw.*, vol. 213, Aug. 2022, Art. no. 109092.

[4] A. S. Cacciapuoti, M. Caleffi, R. Van Meter, and L. Hanzo, "When entanglement meets classical communications: Quantum teleportation for the quantum internet," *IEEE Trans. Commun.*, vol. 68, no. 6, pp. 3808–3833, Jun. 2020.

[5] A. S. Cacciapuoti, M. Caleffi, F. Tafuri, F. S. Cataliotti, S. Gherardini, and G. Bianchi, "Quantum internet: Networking challenges in distributed quantum computing," *IEEE Netw.*, vol. 34, no. 1, pp. 137–143, Jan./Feb. 2019.

[6] S. Wehner, D. Elkouss, and R. Hanson, "Quantum internet: A vision for the road ahead," *Science*, vol. 362, no. 6412, pp. 1–9, Oct. 2018, doi: 10.1126/science.aam9288.

[7] A. Dahlberg and S. Wehner, "SimulaQron—A simulator for developing quantum internet software," *Quantum Sci. Technol.*, vol. 4, no. 1, Sep. 2018, Art. no. 015001.

[8] H. J. Kimble, "The quantum internet," *Nature*, vol. 453, no. 7198, pp. 1023–1030, Jun. 2008.

[9] S. Lloyd, J. H. Shapiro, F. N. C. Wong, P. Kumar, S. M. Shahriar, and H. P. Yuen, "Infrastructure for the quantum internet," *ACM SIGCOMM Comput. Commun. Rev.*, vol. 34, no. 5, pp. 9–20, Oct. 2004.

[10] R. Horodecki, P. Horodecki, M. Horodecki, and K. Horodecki, "Quantum entanglement," *Rev. Mod. Phys.*, vol. 81, no. 2, pp. 865–942, 2009.

[11] G. Vidal and R. F. Werner, "Computable measure of entanglement," *Phys. Rev. A*, vol. 65, no. 3, Feb. 2002, Art. no. 032314.

[12] V. Vedral, M. B. Plenio, M. A. Rippin, and P. L. Knight, "Quantifying entanglement," *Phys. Rev. Lett.*, vol. 78, no. 12, pp. 2275–2279, 1997.

[13] P. W. Shor, "Fault-tolerant quantum computation," in *Proc. 37th Conf. Found. Comput. Sci.*, Los Alamitos, CA, USA, 1996, pp. 56–65.

[14] P. W. Shor, "Algorithms for quantum computation: Discrete logarithms and factoring," in *Proc. 35th Annu. Symp. Found. Comput. Sci.*, Santa Fe, NM, USA, 1994, pp. 124–134.

[15] A. S. Fletcher, P. W. Shor, and M. Z. Win, "Channel-adapted quantum error correction for the amplitude damping channel," *IEEE Trans. Inf. Theory*, vol. 54, no. 12, pp. 5705–5718, Dec. 2008.

[16] A. S. Fletcher, P. W. Shor, and M. Z. Win, "Optimum quantum error recovery using semidefinite programming," *Phys. Rev. A*, vol. 75, no. 1, Jan. 2007, Art. no. 012338.

[17] A. Barenco et al., "Elementary gates for quantum computation," *Phys. Rev. A*, vol. 52, no. 5, pp. 3457–3467, Nov. 1995.

[18] D. Bruß and C. Macchiavello, "Multipartite entanglement in quantum algorithms," *Phys. Rev. A*, vol. 83, no. 5, May 2011, Art. no. 052313.

[19] A. S. Fletcher, P. W. Shor, and M. Z. Win, "Structured near-optimal channel-adapted quantum error correction," *Phys. Rev. A*, vol. 77, no. 1, Jan. 2008, Art. no. 012320.

[20] S. Guerrini, M. Z. Win, M. Chiani, and A. Conti, "Quantum discrimination of noisy photon-added coherent states," *IEEE J. Sel. Areas Inf. Theory*, vol. 1, no. 2, pp. 469–479, Aug. 2020.

[21] Q. Zhuang, Z. Zhang, and J. H. Shapiro, "Distributed quantum sensing using continuous-variable multipartite entanglement," *Phys. Rev. A*, vol. 97, no. 3, Mar. 2018, Art. no. 032329.

[22] Q. Zhuang, Z. Zhang, and J. H. Shapiro, "Optimum mixed-state discrimination for noisy entanglement-enhanced sensing," *Phys. Rev. Lett.*, vol. 118, no. 4, Jan. 2017, Art. no. 040801.

[23] M. Reichert, R. Di Candia, M. Z. Win, and M. Sanz, "Quantum-enhanced Doppler LiDAR," *npj Quantum Inf.*, vol. 8, no. 1, pp. 1–9, Dec. 2022.

[24] G. M. D'Ariano, P. L. Presti, and M. G. A. Paris, "Using entanglement improves the precision of quantum measurements," *Phys. Rev. Lett.*, vol. 87, no. 27, Dec. 2001, Art. no. 270404.

[25] Z. Huang, C. Macchiavello, and L. Maccone, "Usefulness of entanglement-assisted quantum metrology," *Phys. Rev. A*, vol. 94, no. 1, Jul. 2016, Art. no. 012101.

[26] V. Giovannetti, S. Lloyd, and L. Maccone, "Advances in quantum metrology," *Nature Photon.*, vol. 5, no. 4, pp. 222–229, 2011.

[27] V. Giovannetti, S. Lloyd, and L. Maccone, "Quantum-enhanced positioning and clock synchronization," *Nature*, vol. 412, pp. 417–419, Jul. 2001.

[28] S. Marano and M. Z. Win, "Distributing quantum states with finite lifetime," *Phys. Rev. A*, vol. 107, no. 5, May 2023, Art. no. 052413, doi: 10.1103/PhysRevA.107.052413.

[29] M. Chiani, A. Conti, and M. Z. Win, "Piggybacking on quantum streams," *Phys. Rev. A*, vol. 102, no. 1, Jul. 2020, Art. no. 012410.

[30] G. Cariolaro, *Quantum Communications*. Cham, Switzerland: Springer, 2015.

[31] M. He, R. Malaney, and R. Aguinaldo, "Teleportation of discrete-variable qubits via continuous-variable lossy channels," *Phys. Rev. A*, vol. 105, no. 6, Jun. 2022, Art. no. 062407.

[32] E. Villaseñor, M. He, Z. Wang, R. Malaney, and M. Z. Win, "Enhanced uplink quantum communication with satellites via downlink channels," *IEEE Trans. Quant. Eng.*, vol. 2, pp. 1–18, 2021.

[33] N. Hosseinidehaj, Z. Babar, R. Malaney, S. X. Ng, and L. Hanzo, "Satellite-based continuous-variable quantum communications: State-of-the-art and a predictive outlook," *IEEE Commun. Surveys Tuts.*, vol. 21, no. 1, pp. 881–919, 1st Quart., 2019.

[34] S. Lloyd, "Power of entanglement in quantum communication," *Phys. Rev. Lett.*, vol. 90, no. 16, Apr. 2003, Art. no. 167902.

[35] P. Mandayam, K. Jagannathan, and A. Chatterjee, "The classical capacity of additive quantum queue-channels," *IEEE J. Sel. Areas Inf. Theory*, vol. 1, no. 2, pp. 432–444, Aug. 2020.

[36] S. Pirandola, "End-to-end capacities of a quantum communication network," *Commun. Phys.*, vol. 2, no. 1, p. 51, May 2019.

[37] W. Dai, T. Peng, and M. Z. Win, "Optimal remote entanglement distribution," *IEEE J. Sel. Areas Commun.*, vol. 38, no. 3, pp. 540–556, Mar. 2020.

[38] J. Yin et al., "Satellite-based entanglement distribution over 1200 kilometers," *Science*, vol. 356, no. 6343, pp. 1140–1144, Jun. 2017.

[39] J. I. Cirac, P. Zoller, H. J. Kimble, and H. Mabuchi, "Quantum state transfer and entanglement distribution among distant nodes in a quantum network," *Phys. Rev. Lett.*, vol. 78, no. 16, pp. 3221–3224, 1997.

[40] K. Chakraborty, D. Elkouss, B. Rijsman, and S. Wehner, "Entanglement distribution in a quantum network: A multicommodity flow-based approach," *IEEE Trans. Quantum Eng.*, vol. 1, pp. 1–21, 2020.

[41] S. Brand, T. Coopmans, and D. Elkouss, "Efficient computation of the waiting time and fidelity in quantum repeater chains," *IEEE J. Sel. Areas Commun.*, vol. 38, no. 3, pp. 619–639, Mar. 2020.

[42] Á. G. Iñesta, G. Vardoyan, L. Scavuzzo, and S. Wehner, "Optimal entanglement distribution policies in homogeneous repeater chains with cutoffs," *Npj Quantum Inf.*, vol. 9, no. 1, pp. 1–7, May 2023.

[43] B. T. Kirby, S. Santra, V. S. Malinovsky, and M. Brodsky, "Entanglement swapping of two arbitrarily degraded entangled states," *Phys. Rev. A*, vol. 94, no. 1, Jul. 2016, Art. no. 012336.

[44] J.-W. Pan, D. Bouwmeester, H. Weinfurter, and A. Zeilinger, "Experimental entanglement swapping: Entangling photons that never interacted," *Phys. Rev. Lett.*, vol. 80, no. 18, pp. 3891–3894, May 1998.

[45] M. Zukowski, A. Zeilinger, M. A. Horne, and A. K. Ekert, "'Event-ready-detectors' Bell experiment via entanglement swapping," *Phys. Rev. Lett.*, vol. 71, no. 26, pp. 4287–4290, 1993.

[46] M. A. Nielsen and I. L. Chuang, *Quantum Computation and Quantum Information*. Cambridge, U.K.: Cambridge Univ. Press, 2000.

[47] R. Jozsa, "Fidelity for mixed quantum states," *J. Mod. Optic*, vol. 41, no. 12, pp. 2315–2323, 1994.

[48] Y.-C. Liang, Y.-H. Yeh, P. E. M. F. Mendonça, R. Y. Teh, M. D. Reid, and P. D. Drummond, "Quantum fidelity measures for mixed states," *Rep. Prog. Phys.*, vol. 82, no. 7, Jul. 2019, Art. no. 076001.

[49] T. Opatrný and G. Kurizki, "Optimization approach to entanglement distillation," *Phys. Rev. A*, vol. 60, no. 1, pp. 167–172, Jul. 1999.

[50] C. H. Bennett, D. P. DiVincenzo, J. A. Smolin, and W. K. Wootters, "Mixed-state entanglement and quantum error correction," *Phys. Rev. A*, vol. 54, no. 5, pp. 3824–3851, Nov. 1996.

[51] D. Deutsch, A. Ekert, R. Jozsa, C. Macchiavello, S. Popescu, and A. Sanpera, "Quantum privacy amplification and the security of quantum cryptography over noisy channels," *Phys. Rev. Lett.*, vol. 77, no. 13, pp. 2818–2821, Sep. 1996, doi: 10.1103/PhysRevLett.77.2818.

[52] C. H. Bennett, G. Brassard, S. Popescu, B. Schumacher, J. A. Smolin, and W. K. Wootters, "Purification of noisy entanglement and faithful teleportation via noisy channels," *Phys. Rev. Lett.*, vol. 76, no. 5, pp. 722–725, Jan. 1996.

[53] L. Ruan, W. Dai, and M. Z. Win, "Adaptive recurrence quantum entanglement distillation for two-Kraus-operator channels," *Phys. Rev. A*, vol. 97, no. 5, May 2018, Art. no. 052332, doi: 10.1103/PhysRevA.97.052332.

[54] L. Ruan, B. T. Kirby, M. Brodsky, and M. Z. Win, "Efficient entanglement distillation for quantum channels with polarization mode dispersion," *Phys. Rev. A*, vol. 103, no. 3, Mar. 2021, Art. no. 032425, doi: 10.1103/PhysRevA.103.032425.

[55] E. Shchukin and P. van Loock, "Optimal entanglement swapping in quantum repeaters," *Phys. Rev. Lett.*, vol. 128, no. 15, Apr. 2022, Art. no. 150502.

[56] S. B. V. Dam, P. C. Humphreys, F. Rozpedek, S. Wehner, and R. Hanson, "Multiplexed entanglement generation over quantum networks using multi-qubit nodes," *Quantum Sci. Technol.*, vol. 2, no. 3, Sep. 2017, Art. no. 034002.

[57] M. Caleffi, "Optimal routing for quantum networks," *IEEE Access*, vol. 5, pp. 22299–22312, 2017.

[58] M. Pant et al., "Routing entanglement in the quantum internet," *NPJ Quantum Inf.*, vol. 5, no. 1, pp. 1–9, Mar. 2019, doi: 10.1038/s41534-019-0139-x.

[59] N. K. Bernardes, L. Praxmeyer, and P. van Loock, "Rate analysis for a hybrid quantum repeater," *Phys. Rev. A*, vol. 83, no. 1, Jan. 2011, Art. no. 012323.

[60] J. Li et al., "Fidelity-guaranteed entanglement routing in quantum networks," *IEEE Trans. Commun.*, vol. 70, no. 10, pp. 6748–6763, Oct. 2022.

[61] W. Dür, H.-J. Briegel, J. I. Cirac, and P. Zoller, "Quantum repeaters based on entanglement purification," *Phys. Rev. A*, vol. 59, no. 1, pp. 169–181, 1999.

[62] H.-J. Briegel, W. Dur, J. I. Cirac, and P. Zoller, "Quantum repeaters: The role of imperfect local operations in quantum communication," *Phys. Rev. Lett.*, vol. 81, no. 26, pp. 5932–5935, Dec. 1998.

[63] Z. Liu, S. Marano, and M. Z. Win, "An asymptotically achievable rate bound for establishing high-fidelity entanglements in quantum networks," in *Proc. IEEE Int. Conf. Acoust., Speech Signal Process. (ICASSP)*, Apr. 2024, pp. 1–5.

[64] M. Shtaif, C. Antonelli, and M. Brodsky, "Nonlocal compensation of polarization mode dispersion in the transmission of polarization entangled photons," *Opt. Exp.*, vol. 19, no. 3, p. 1728, 2011, doi: 10.1364/oe.19.001728.

[65] C. Antonelli, M. Shtaif, and M. Brodsky, "Sudden death of entanglement induced by polarization mode dispersion," *Phys. Rev. Lett.*, vol. 106, no. 8, Feb. 2011, Art. no. 080404, doi: 10.1103/physrevlett.106.080404.

[66] M. Brodsky, E. C. George, C. Antonelli, and M. Shtaif, "Loss of polarization entanglement in a fiber-optic system with polarization mode dispersion in one optical path," *Opt. Lett.*, vol. 36, no. 1, pp. 43–45, 2011, doi: 10.1364/ol.36.000043.

[67] B. Li, T. Coopmans, and D. Elkouss, "Efficient optimization of cutoffs in quantum repeater chains," *IEEE Trans. Quantum Eng.*, vol. 2, pp. 1–15, 2021.

[68] S. Khatri, C. T. Matyas, A. U. Siddiqui, and J. P. Dowling, "Practical figures of merit and thresholds for entanglement distribution in quantum networks," *Phys. Rev. Res.*, vol. 1, no. 2, Sep. 2019, Art. no. 023032.

[69] F. Rozpedek et al., "Parameter regimes for a single sequential quantum repeater," *Quantum Sci. Technol.*, vol. 3, no. 3, Apr. 2018, Art. no. 034002.

[70] P. van Loock et al., "Extending quantum links: Modules for fiber- and memory-based quantum repeaters," *Adv. Quantum Technol.*, vol. 3, no. 11, Nov. 2020, Art. no. 1900141.

[71] S. Bratzik, S. Abruzzo, H. Kampermann, and D. Bruß, "Quantum repeaters and quantum key distribution: The impact of entanglement distillation on the secret key rate," *Phys. Rev. A*, vol. 87, no. 6, Jun. 2013, Art. no. 062335.

[72] S. Abruzzo, S. Bratzik, N. K. Bernardes, H. Kampermann, P. van Loock, and D. Bruß, "Quantum repeaters and quantum key distribution: Analysis of secret-key rates," *Phys. Rev. A*, vol. 87, no. 5, May 2013, Art. no. 052315.

[73] X.-M. Hu et al., "Long-distance entanglement purification for quantum communication," *Phys. Rev. Lett.*, vol. 126, no. 1, Jan. 2021, Art. no. 010503.

[74] Y. Jing, D. Alsina, and M. Razavi, "Quantum key distribution over quantum repeaters with encoding: Using error detection as an effective postselection tool," *Phys. Rev. Appl.*, vol. 14, no. 6, Dec. 2020, Art. no. 064037.

[75] V. Scarani, H. Bechmann-Pasquinucci, N. J. Cerf, M. Dušek, N. Lütkenhaus, and M. Peev, "The security of practical quantum key distribution," *Rev. Mod. Phys.*, vol. 81, pp. 1301–1350, Sep. 2009.

[76] Y. Jing and M. Razavi, "Simple efficient decoders for quantum key distribution over quantum repeaters with encoding," *Phys. Rev. Appl.*, vol. 15, no. 4, Apr. 2021, Art. no. 044027.

[77] A. Patil, M. Pant, D. Englund, D. Towsley, and S. Guha, "Entanglement generation in a quantum network at distance-independent rate," *Npj Quantum Inf.*, vol. 8, no. 1, May 2022.

[78] S. Pouryousef, N. K. Panigrahy, and D. Towsley, "A quantum overlay network for efficient entanglement distribution," in *Proc. IEEE INFOCOM Conf. Comput. Commun.*, New York, NY, USA, May 2023, pp. 1–10.

[79] Z. Xiao et al., "A connectionless entanglement distribution protocol design in quantum networks," *IEEE Netw.*, early access, Oct. 9, 2024, doi: 10.1109/MNET.2023.3321044.

[80] D. B. West, *Introduction to Graph Theory*, vol. 2. Upper Saddle River, NJ, USA: Prentice-Hall, 1996.

[81] L. A. Shepp, "Private conversation," Lucent Bell Lab. Res., Tech. Rep., Jul. 1999.

[82] M. S. Klamkin and D. J. Newman, "The philosophy and applications of transform theory," *SIAM Rev.*, vol. 3, no. 1, pp. 10–36, 1960.

[83] M. Z. Win and J. H. Winters, "Virtual branch analysis of symbol error probability for hybrid selection/maximal-ratio combining in Rayleigh fading," *IEEE Trans. Commun.*, vol. 49, no. 11, pp. 1926–1934, Nov. 2001.
[84] W. Suwansantisuk and M. Z. Win, "Multipath aided rapid acquisition: Optimal search strategies," *IEEE Trans. Inf. Theory*, vol. 53, no. 1, pp. 174–193, Jan. 2007.
[85] D. P. Bertsekas, *Dynamic Programming and Optimal Control: Volume I*, 4th ed. Belmont, MA, USA: Athena Scientific, 2017.
[86] D. P. Bertsekas, *Dynamic Programming and Optimal Control: Volume II*, 4th ed. Belmont, MA, USA: Athena Scientific, 2012.
[87] D. P. Bertsekas, *Reinforcement Learning and Optimal Control*, 1st ed. Belmont, MA, USA: Athena Scientific, 2019.
[88] P. R. Kumar and P. Varaiya, *Stochastic Systems: Estimation, Identification, and Adaptive Control*. Englewood Cliffs, NJ, USA: Prentice-Hall, 1986.
[89] V. S. Borkar and S. K. Mitter, "LQG control with communication constraints," in *Communications, Computation, Control, and Signal Processing: A Tribute to Thomas Kailath*, A. Paulraj, V. Roychowdhury, and C. D. Schaper, Eds. New York, NY, USA: Springer, 1997, pp. 365–373.
[90] T. Tanaka, P. M. Esfahani, and S. K. Mitter, "LQG control with minimum directed information: Semidefinite programming approach," *IEEE Trans. Autom. Control*, vol. 63, no. 1, pp. 37–52, Jan. 2018.
[91] P. Billingsley, *Probability and Measure*, 3rd ed. New York, NY, USA: Wiley, 1995.
[92] D. Bertsimas and J. N. Tsitsiklis, *Introduction to Linear Optimization*, 1st ed. Belmont, MA, USA: Athena Scientific, 1997.
[93] D. P. Bertsekas, *Convex Optimization Theory*. Belmont, MA, USA: Athena Scientific, 2009.
[94] G. B. Dantzig, *Linear Programming and Extensions*. Princeton, NJ, USA: Princeton Univ. Press, 1963.
[95] S. Marano and M. Z. Win, "Distillation and swapping for quantum dragonflies," Lab. Inf. Decis. Syst. (LIDS), Massachusetts Inst. Technol., Prog. Rep. LIDS-P-3435, Apr. 2024.
[96] D. S. Gunderson, *Handbook of Mathematical Induction: Theory and Applications*, 1st ed. Boca Raton, FL, USA: Chapman, 2010.
[97] R. Durrett, *Probability: Theory and Examples*, 5th ed. New York, NY, USA: Cambridge Univ. Press, 2019.

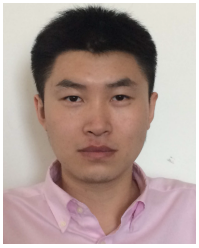

Zhenyu Liu (Member, IEEE) received the Ph.D. degree in networks and statistics and the S.M. degree in aeronautics and astronautics both from the Massachusetts Institute of Technology (MIT) in 2022. He received the M.S. degree and the B.S. degree (with honor) in electronic engineering from Tsinghua University, Beijing, China, in 2014 and 2011, respectively.

Since 2022, he has been a Post-Doctoral Associate in the wireless information and network sciences laboratory at MIT. His research interests include wireless communications, network localization, distributed inference, networked control, and quantum information science.

Dr. Liu received the first prize of the IEEE Communications Society's Student Competition in 2019 and 2016, the Research and Development 100 Award for Peregrine System in 2018, and the Best Paper Award at the IEEE Latin-American Conference on Communications in 2017.

Stefano Marano (Senior Member, IEEE) received the Ph.D. degree in electronic engineering and computer science and the Laurea degree (summa cum laude) in electronic engineering, both from the University of Naples, Italy, in 1997 and 1993, respectively.

He is a Professor at Department of Information & Electrical Engineering and Applied Mathematics, University of Salerno, Italy. He has been a frequent visitor to the Wireless Information and Network Sciences Laboratory at the Massachusetts Institute of Technology, where he presently holds the Research Affiliate appointment. He held visiting positions at Department of Electrical and Computer Engineering, University of California at San Diego, CA, USA, and at Physics Department, University of Wales, College of Cardiff, UK, in 2013 and 1996, respectively. His research interests include decision theory, distributed inference, information theory, and quantum information science. He has co-authored more than 100 journal articles and has given several invited talks at universities and international research centers.

Prof. Marano was awarded the IEEE TRANSACTIONS ON ANTENNAS AND PROPAGATION best paper award in 1999 for his work on stochastic modeling of electromagnetic propagation in urban environments. He was in the organizing committee of the IEEE radar conference (RADARCON 2008) and of the ninth international conference on information fusion (FUSION 2006). He served as associate editor and technical editor for the IEEE TRANSACTIONS ON AEROSPACE AND ELECTRONIC SYSTEMS (2009-2016) and associate editor for the IEEE TRANSACTIONS ON SIGNAL PROCESSING (2010-2014).

Moe Z. Win (Fellow, IEEE) is a Professor at the Massachusetts Institute of Technology (MIT) and the founding director of the Wireless Information and Network Sciences Laboratory. Prior to joining MIT, he was with AT&T Research Laboratories and with NASA Jet Propulsion Laboratory.

His research encompasses fundamental theories, algorithm design, and network experimentation for a broad range of real-world problems. His current research topics include ultra-wideband systems, network localization and navigation, network interference exploitation, and quantum information science. He has served the IEEE Communications Society as an elected Member-at-Large on the Board of Governors, as elected Chair of the Radio Communications Committee, and as an IEEE Distinguished Lecturer. Over the last two decades, he held various editorial positions for IEEE journals and organized numerous international conferences. Recently, he served on the SIAM Diversity Advisory Committee.

Dr. Win is an elected Fellow of the AAAS, the EURASIP, the IEEE, and the IET. He was honored with two IEEE Technical Field Awards: the IEEE Kiyo Tomiyasu Award (2011) and the IEEE Eric E. Sumner Award (2006, jointly with R. A. Scholtz). His publications, co-authored with students and colleagues, have received several awards. Other recognitions include the MIT Everett Moore Baker Award (2022), the IEEE Vehicular Technology Society James Evans Avant Garde Award (2022), the IEEE Communications Society Edwin H. Armstrong Achievement Award (2016), the Cristoforo Colombo International Prize for Communications (2013), the Copernicus Fellowship (2011) and the *Laurea Honoris Causa* (2008) both from the Università degli Studi di Ferrara, and the U.S. Presidential Early Career Award for Scientists and Engineers (2004).